No. 149 THE NORTHEAST RIM OF TYCHO

by RALPH J. TURNER

March 25, 1970

ABSTRACT

The construction and interpretation of a scale relief model of the NE Rim of Tycho are described. The region is the first of two adjacent areas selected for their uncommon interest, owing to the presence of numerous "lava lakes" that occur at different levels in the outer walls of the crater and the "Pebble" described by Dr. Kuiper in Appendix I. The boundaries of this first model are 8°30′ to 9°30′ W and 42°15′ to 42°55′ S. Its scale is 1:20,000, the lateral resolution better than 60 meters, and the vertical sensitivity about 20 meters. A collimated light beam, 45 × 125 cm, was produced by two large Fresnel lenses. Adjustable orientations were provided in two coordinates, as required by the different lighting conditions of the original records, *Orbiter* and Earth-based (Fig. 4). Elevational and albedo control on the larger scale is based on 17 telescopic photographs (all but one taken with the 61-inch telescope); coordination and detail relies on five *Orbiter IV* and *V* frames. Figs. 3, 9, 15, 19, and 31 show the completed model.

The paper includes photographs of the model compared to copies of original records, allowing the reader to verify its overall validity. The model was measured with a special device (Fig. 10), yielding a total of over 150,000 relief points, from which a topographic map was derived having 20-meter contour intervals. This topographic map is inserted as *Map A*. It is accompanied by *Map B*, a relief contour map, that will assist in the interpretation of the photographic records. The model area covers 450 km^2 of lunar highland. Lava lakes are found at various elevations, ranging over 2000 meters. In some cases the lakes are interconnected. Slope angles vary from 0° to 36°. Impact craters are few in number. The rim of Tycho and two rough-textured hills have above-average albedos.

Our procedures integrate formation from a variety of sources that on first inspection may appear contradictory; and present it in numerical form for further geophysical interpretation.

The three Appendices give supplementary information, on the Pebble, on crater counts, and on dimple craters, respectively.

1. Earlier Models

In connection with the LPL responsibilities in the study of *Ranger VI-IX* records, the author was invited in 1964 to initiate, on a part-time basis, a program of modeling lunar reliefs. The first terrain studied was the impact area of *Ranger VII* on Mare Cognitum. While the immediate aim was to clarify the nature of the linear features and shallow craters recorded, it was soon found that these more-obvious features were contained in a less-obvious undulating terrain representing substantial volumes (Kuiper, 1965*a;* Kuiper, 1965*b;* Kuiper, 1966, and Turner, 1966).

The following year, with an improved lighting system, a scale model was undertaken of Alphonsus' central peak recorded by *Ranger IX* (JPL-NASA *Ranger VIII-IX* Report).

In addition, the author modeled a few lunar dimple craters, later accompanied by a model of a terrestrial collapse depression, roughly surveyed and explored during an LPL field trip organized by Dr. Kuiper early in 1966 in which the author participated. These results are summarized in Appendix III.

The author developed from 1966 to 1968 on a part-time basis, a model of the NE rim of Alphonsus under improved lighting conditions, based on com-

plementary photo records from *Ranger IX* and *Orbiter IV*. Some problems arose in determining the gross relief dimensions that were never satisfactorily solved for lack of adequate data. As a result, this model exists only in a "proof" form, but the intensive study given the area has aided comparison with the Tycho rim model. One conclusion was that the inner slope of Alphonsus is not "terraced" but consists of a series of concentric ridges.

2. *The Tycho Region*

The *Orbiter IV* and *V* missions revealed two most interesting aspects of the Tycho area: (1) the *roughness* of the Tycho floor, entirely different from what was expected from simple impact; (2) several *lava lakes,* both on the inner and outer walls, in contrast with the cracked and wrinkled ridges of the floor. The lakes are especially extensive on the outer slopes. In consultation with Dr. Kuiper a portion of the Tycho rim was selected for modeling, of sufficient size to include several "lakes" but not so large as to prevent all recorded data to be entered in a model of manageable dimensions; the adjacent rim area, containing the "Pebble" (cf. Appendix I) will be treated next.

The shapes of the lakes are clearly related to the arcuate and linear terrain features. There is a paucity of large craters. A few sharp-appearing cracks or faults accompany the lakes. Tycho generally, and this region particularly, was identified as a "hot spot" by Saari and Shorthill (1966), indicating *exposed rock*. The Tycho ray system begins outside the dark halo surrounding the crater; *the model lies within the dark halo* and *no rays* are present within its boundaries.

The model was designed to combine all available topographic detail in the area covered. While for its detailed topography based on the *Orbiter* records, 17 plates and some visual observations with the 61-inch telescope were used also for the overall level differences and albedos. It extends from 8°30′ to 9°30′ W longitude, and 42°15′ to 42°55′ S latitude.

Special emphasis was directed toward determining the relative *lake levels,* which required accurate modeling; and the relationship of the lakes to the main structural elements of the Tycho Rim.

3. *Modeling Procedure*

Four *Orbiter V* "medium resolution" frames were available in September 1968; M125-M128. Pairs of these yielded good stereo views. Inspection was facilitated when accurate coordinates were drawn. It was then discovered that on the records issued, the individual framelets had been trimmed narrow, which had removed information that was recoverable from the other frames (cf. Fig. 2). The individual strips were re-mounted over their complements from other frames, which made coordination consistent, and improved the stereo effect.

In the spacecraft every other strip within a frame had been focused on alternate sides of the film which resulted in slightly different resolutions. One task was therefore to place the frames appropriately by inspection of alternate sets having different boundary cuts.

The smallest craters and rocks identifiable on the *Orbiter* records measured about 50 meters. The solar altitude at the center of the model, 9° W, 42°35′ S, was 11°1; the azimuth 12°1 N of E.

Fourteen 61-inch photographs of Tycho were available when the project began. Their value lay in their span of sun elevations:

CATALINA PHOTOGRAPHS USED

Designation	Sun Altitude	Sun Azimuth
314	12°3	11° N of E
483	33°	35°5 N of E
838 (Fig. 30)	6°2	4° N of E
1161	11°	8° N of E
1919	0°8	1° N of E
1998	9°6	9° N of E
2435 (Fig. 30)	10°7	12° N of W
2618	22°7	25° N of W
2655	14°6	16° N of W
2681 (Fig. 7)	5°8	7° N of W
3331	43°5	63°5 N of E
3911	8°2	5° N of E
4114 (Fig. 30)	3°3	1° N of E
4203	12°3	11° N of E

Three 61-inch film strips were taken specifically for the model:

Designation	Sun Altitude	Sun Azimuth
Roll 9, 12	43°6	67°6 N of E
Roll 9, 21	38°9	53° N of E
Roll 23, 19	5°	2° N of E

Finally, a good full-moon 61-inch plate, C4475, was obtained in September 1969, with solar altitude 47°5 and azimuth 83° N of W (Fig. 1), not to mention lesser records. One Lick 120-inch plate, ECD 27, was used, with solar altitude 26°7 and azimuth 29°8 N of W.

In addition, the author made, on several nights,

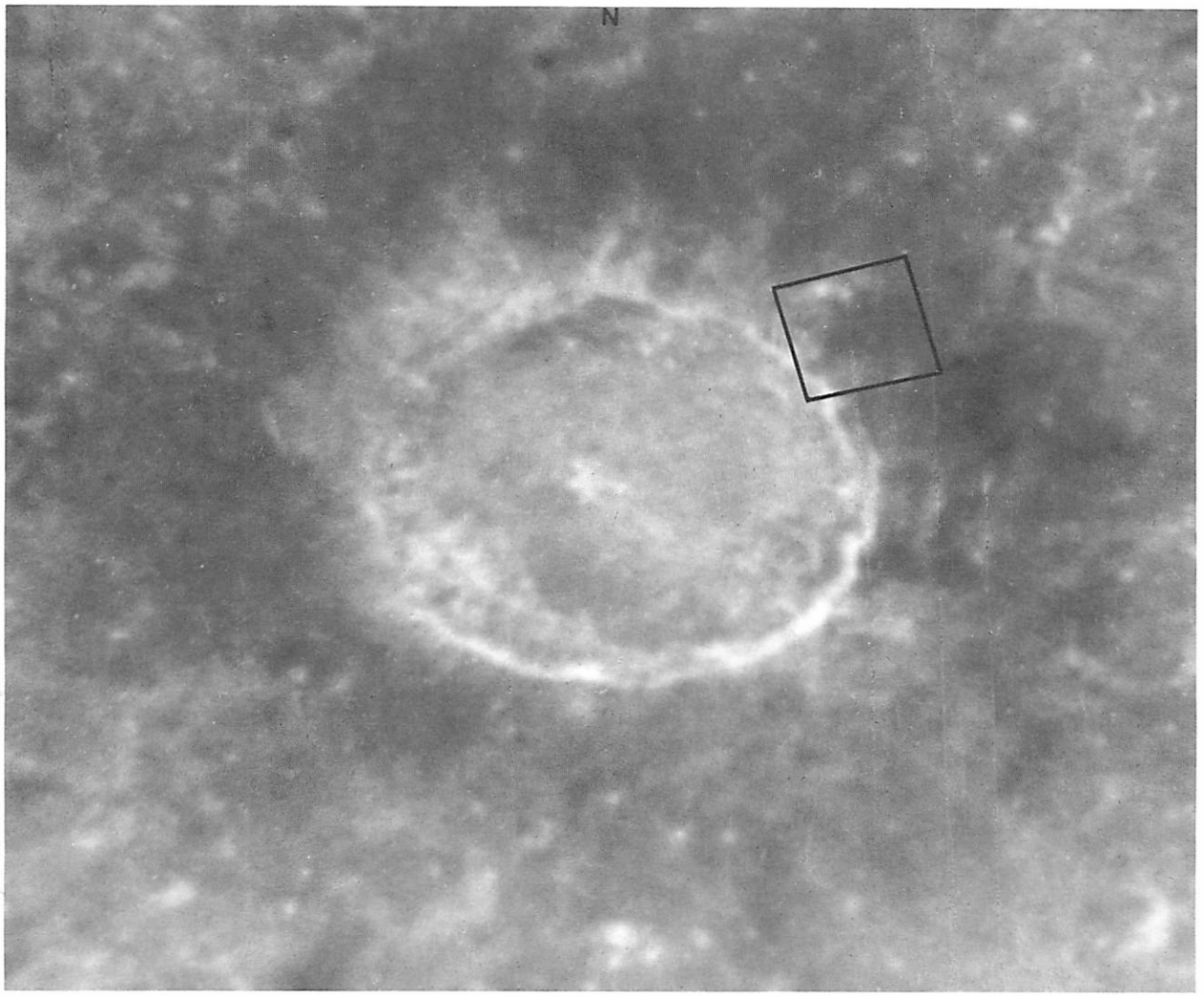

Fig. 1 Catalina 61″ #4475 "Full Moon" photograph (⊙ altitude 47°5, ⊙ azimuth 83° N of W). Note bright central peaks and rim; dark halo, outside which ray system begins. Area of model outlined.

visual observations with the 61-inch to estimate the times when various slopes fell into shadow, as a check on slope angles and thus the elevations of gross features. He also checked albedos, making possible the identification of specific features being especially bright or dark.

The coordination of these records took much time. First, with the assistance of Mr. E. Whitaker, the *Orbiter IV* frame H119 was coordinated from the longitude-latitude overlay of the *Rectified Lunar Atlas* sheet 24a. This was later checked against the U.S. Air Force *Lunar Chart LAC* 112. Then *Orbiter V* frame M125 was inscribed with coordinates from the *Orbiter IV* frame and divided into 5′ intervals (Fig. 2).

The necessary task of coordinating the telescopic records was done with difficulty because of their much lower resolution and of large shadow shifts from one illumination and libration to another. Several successive approximations had to be made. This difficulty was greatest near full moon because of *albedo* areas not obviously corresponding to *relief* features.

In order to re-create the conditions of illumination for each record, it was necessary to control the *lighting and orientation* of the base on which the model was being built. A nearly-parallel light source for a large area was realized by using two 18″ × 24″ Fresnel lenses, each provided with a bright-but-small spherical source at the focus. Stray light was kept to a minimum by using baffles and working in an otherwise dark room. The area of parallel light is thus 18″ × 48″, in which the model could be rotated for matching each photographic record. The finite

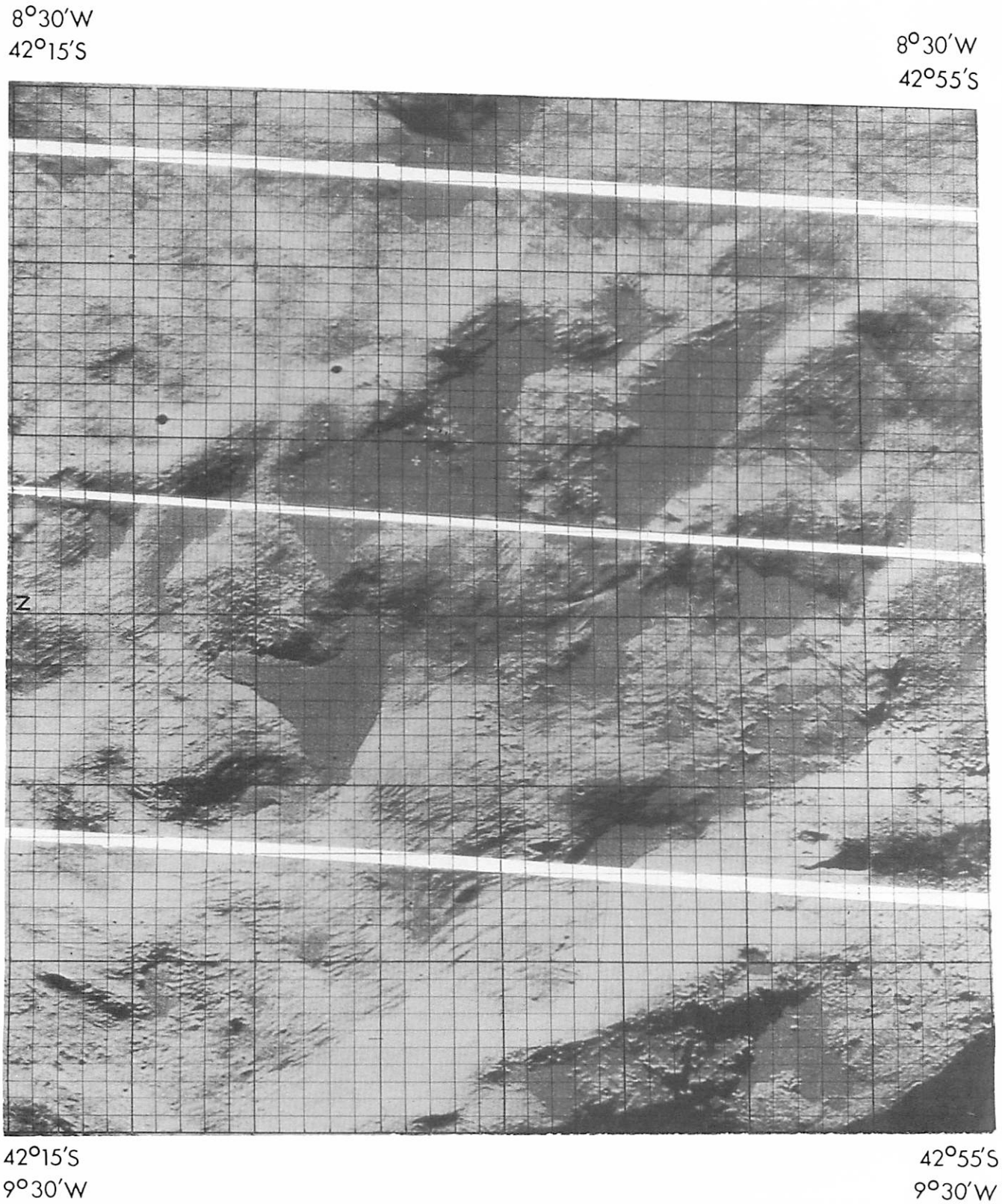

Fig. 2 Orbiter V Photograph, Medium Resolution frame M 125. Coordinates drawn on correctly-spaced strips (⊙ altitude 11°1, ⊙ azimuth 12°1 N of E).

Fig. 3 Relief Model of NE rim of Tycho, under illumination simulating *Orbiter V* (⊙ altitude 11°, ⊙ azimuth 12° N of E).

light sources caused 3°.5 of diffusion, 7 times that by the solar disk. This was not serious; the resulting tendency to slightly shorten the shadows and thus raise the elevations in the model was controlled by the use of different illuminations.

The model is shown in final form in Fig. 3 (and other figures below) and may be compared with the *Orbiter* records, Fig. 2. It was built up of clay on a rigid base plate mounted on an easel that stands perpendicular to the floor. The base plate is turned on center to obtain the different *azimuths* required. The light box is turned so as to simulate the correct local *sun elevation*. The simulated solar azimuths and elevations are measured with devices mounted over the center of the model (Fig. 4).

The solar altitude (h) and azimuth (z) at a lunar position with known longitude (n), latitude (L), solar colongitude ($C_\odot$) and latitude ($b_\odot$), are:

$$\sin h = \cos (90^\circ - b_\odot) \cos (90^\circ - L) + \sin (90^\circ - b_\odot) \sin (90^\circ - L) \sin t$$

and

$$\sin z = -\cos b_\odot \cos t / \cos h,$$

where $t = C_\odot + n$.

To lay out the area to be modeled on the plate, it is assumed that the plate is normal to the radius of the sphere that cuts the surface at 9° W, 42°35′ S. The area of the model is 1.125 m², representing 450 km² on the Moon. Curvature was neglected in measuring coordinates, but in the relief it is automatically allowed for by the illumination. The model then is, in principle, a scale representation of part of the Moon (Fig. 5).

As clay was applied under the parallel beam, the shadow lengths and photometric values of the lunar photographs were being matched by the model. This process is very sensitive to changes of illumination, as is seen in comparing photographs of the model at various sun altitudes, especially low altitudes. Since Tycho is located at a high latitude, there is a large effect of azimuth changes at higher solar altitudes. This allows checking on relative elevations of points not necessarily E or W of each other.

With the illumination used, the *sensitivity of the vertical changes* in elevation was about 0.2 mm (4 meters on the Moon). The control over the horizontal coordination is closer to 1 mm (20 meters on the Moon). Within the available time (some 1,000

Fig. 4 Altitude and azimuth indicators, in place over model. Note model frame, also parallism of beams from Fresnel lenses. Shadows are very dark, as on moon.

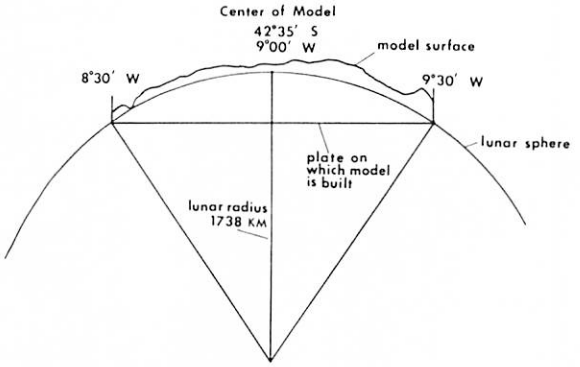

Fig. 5 Diagram of model coordination.

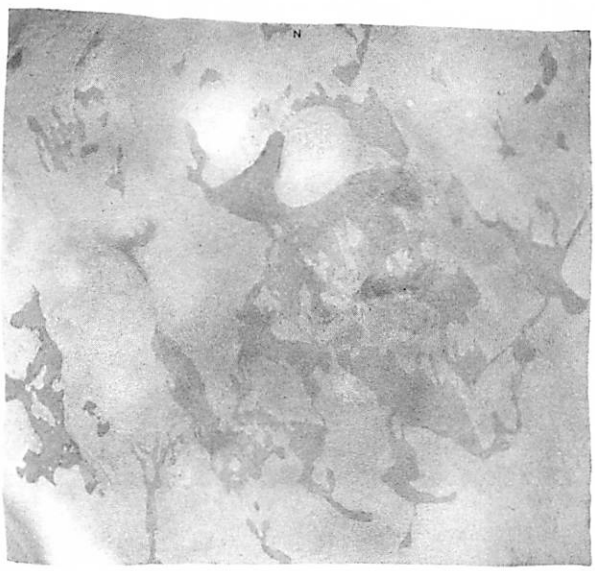

Fig. 6 "Full Moon" photograph of the relief model.

hours were spent on the project), the full resolution obtainable from *Orbiter V* was not achieved everywhere on the model. Generally, an attempt was made to maintain a *horizontal resolution* of about 3 mm (60 m on the Moon) and a vertical sensitivity of 0.5 mm. Interruptions occurred principally in areas of shadow or "burned out" on the *Orbiter V* photos. Fortunately, these areas cover less than 10%. Telescopic views cannot, of course, make up for this loss of good coverage. Thus, while the *detail* within these steeper areas is missing, their elevations, slopes, and general character will be valid.

The *albedos* on the lunar surface are not well known. At the resolution obtainable at the telescope they range from 5-20%. Near full moon, the differences are maximum, but relief is uncertain. At low illuminations the albedo differences almost disappear. In the past this effect was attributed to the peculiar lunar material. However, it is observed also on the model! Thus, relief can be developed without knowledge of the albedo if low-illumination records are available. However, *the problem of correlating full-moon photographs and low-illumination Orbiter records is difficult.* It was attempted, by transferring coordinates from the *Orbiter* records to similarly-illuminated low-resolution records and then, step by step, to full-moon records. Above 15° solar altitude, albedo differences affect the derivation of relief. A hill with high reflectivity will appear unduly high and steep. For this reason, the model was shaded as well as possible to match the albedos on Earth-based photographs; but poor resolution makes the matching of shades to features smaller than 1 km uncertain. Fig. 1 shows the best Earth-based full-moon photo obtained; and Fig. 6, a somewhat shaded photo of the model.

As a check on the method used in developing relief, some *shadow measurements* from telescopic records were made, though this method is of questionable value in complex terrain. For instance, on C2681 it appears as if a shadow falls from a point on the Tycho rim onto L15 (cf. Figs. 7 and 8; the lake numbers are identified in Fig. 16). With the aid of the model it appears that the shadow instead falls on the slope between L14 and L15 (Fig. 7). Because of this ambiguity, measurement of the height of the rim at A above areas B or B′ is unreliable (Fig. 8). It has been our experience that the model can, with due effort, reconcile various seemingly contradictory records and thus serve to integrate all available evidence. Fig. 9 shows the model with illumination matching Fig. 7 and the profile of Fig. 8.

Features lying *outside* the model area sometimes cast shadows on the Moon *within* the model area (though of course not on the model) (Fig. 7, on N boundary of square).

An illusion is produced in the elevation of L13 by the surroundings. Bounded on all sides by high elevations, of great extent on the W and to a lesser extent on the other sides, this feature appears to be unduly low. Through extensive testing, L13 has been found to be lower than L19 but higher than L20, L14 and L15. The effect is best explained by the association of the rise immediately to the E which gives the impression that L13 lies at the bottom of a deep depression. Actually, that broad ridge does not rise very high and drops further on the E to place L14 lower than L13. This illusion is given in the

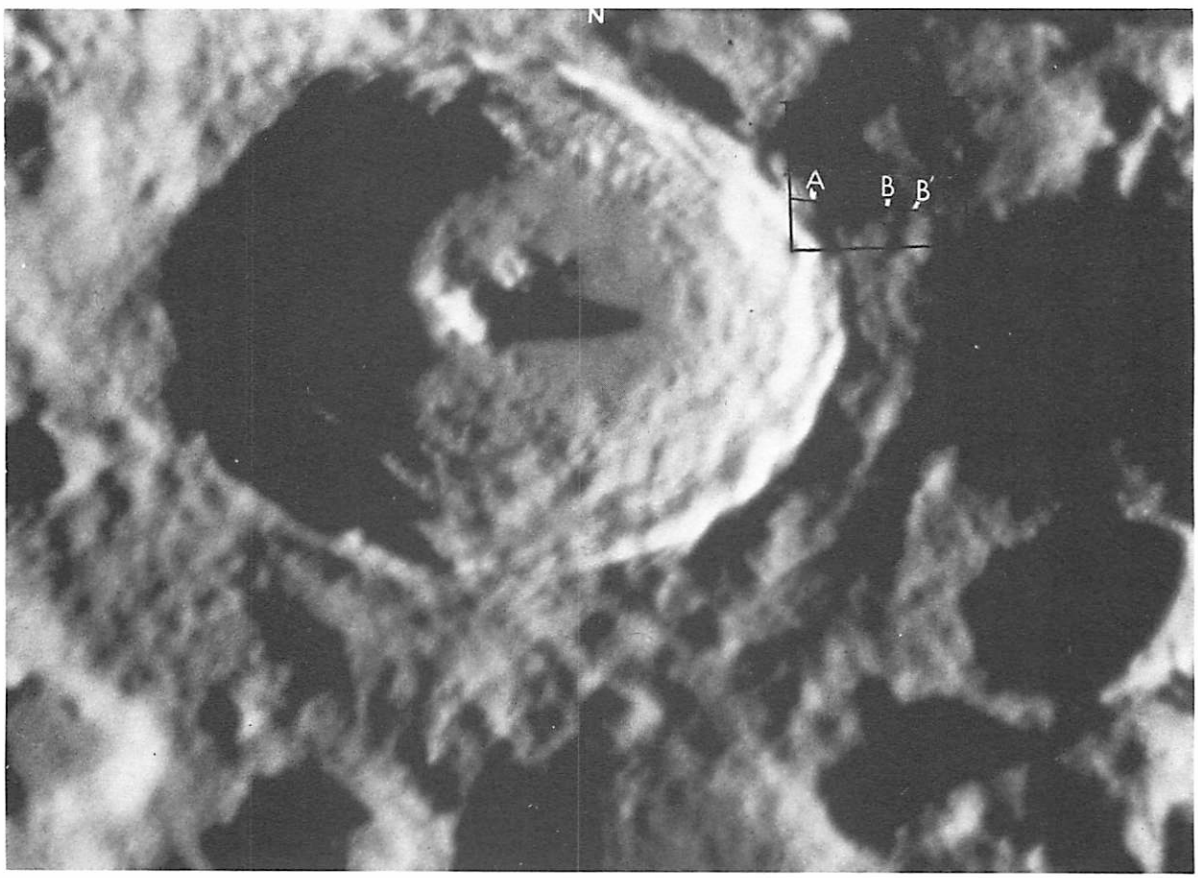

Fig. 7 Catalina 61″ #2681 with shadow-measuring points indicated (⊙ altitude 5°8, ⊙ azimuth 7° N of W).

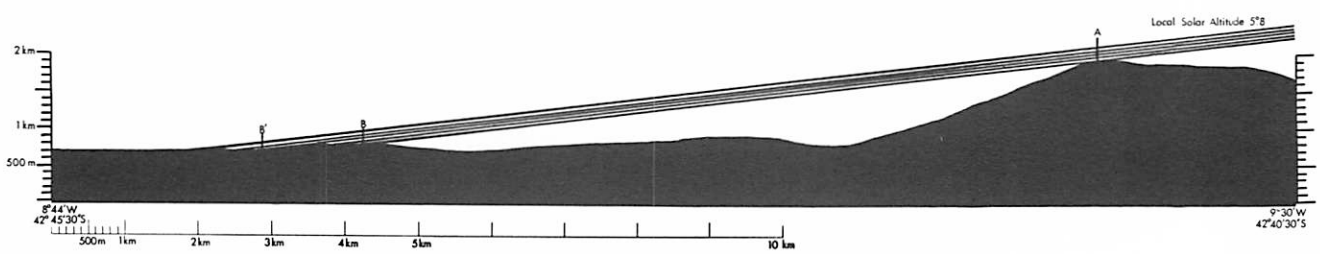

Fig. 8 Cross section taken from the model showing the illumination in Fig. 7 (C2681).

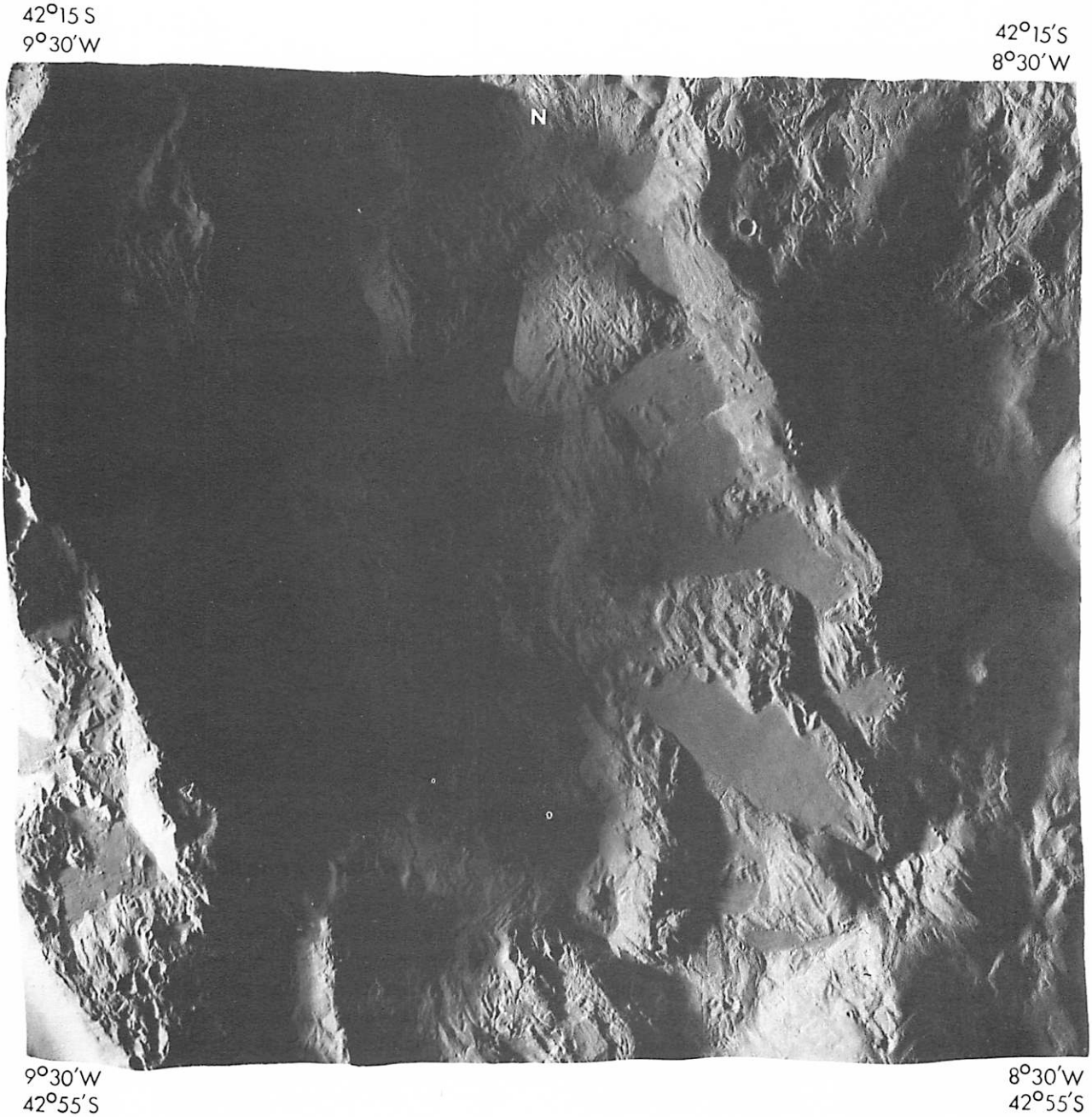

Fig. 9 Relief Model under illumination of C2681 (Fig. 7). (⊙ altitude 6°, ⊙ azimuth 7° N of W).

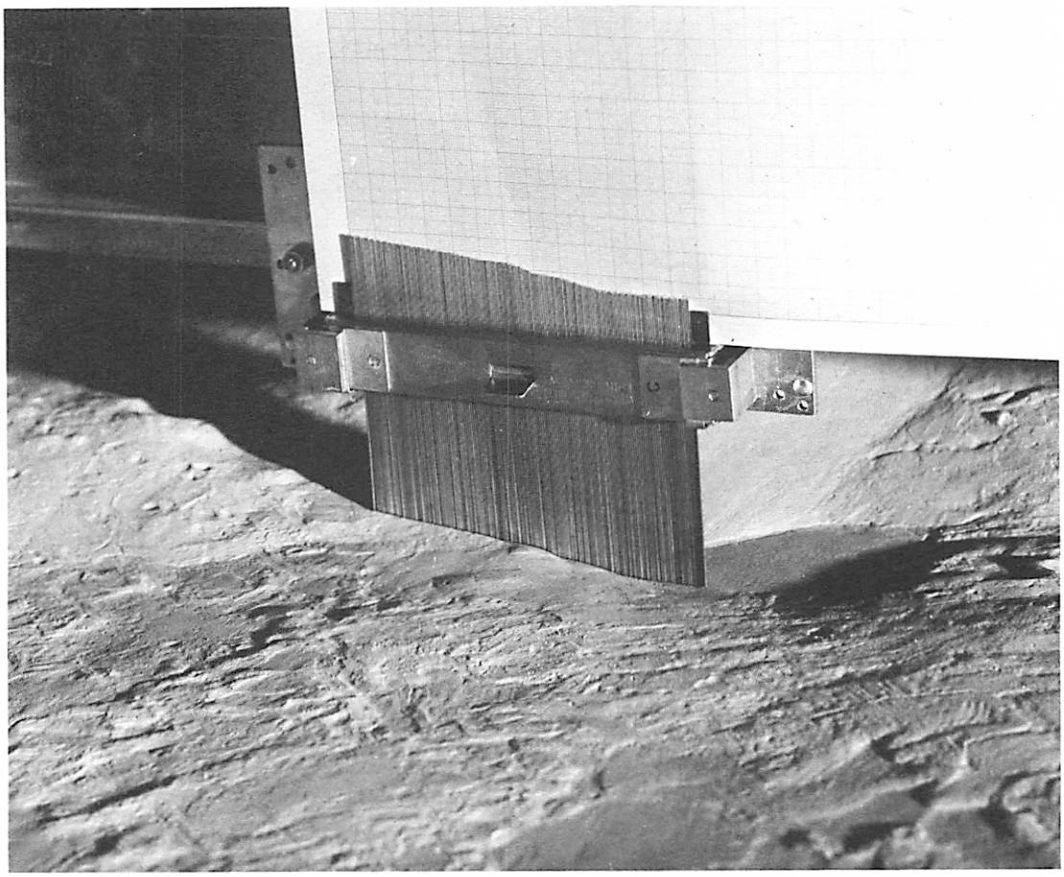

Fig. 10 Elevation and contour-measuring device, in place over model.

stereo viewing of *Orbiter* frames M125-M128, and in stereo views of the model even though measurements place L13 higher than the other lakes. (See stereo view of the model in Fig. 15).

During the modeling, elevations were checked by using a contour-measuring device placed over the model. It consists of 160 rods (1/32 of an inch in diameter and 4 inches long) which are pressed down to the model's surface. Thereupon, one draws a graph over the upper ends of the rods which then corresponds accurately to the contour of the model (cf. Fig. 10). After the model was completed and cast in hydracal, 120 N-S runs on the cast were registered on graphs each 101 cm long, together yielding measures of 153,600 points. From these a *topographic map* was developed *(Map A)*, on which is based *a relief contour map,* also reproduced *(Map B).*

4. Observations From Records And Model

a. The large features — About 13 km of Tycho's rim is contained within the model area but only a small section of the inner slope. This slope was in shadow when *Orbiter* passed. Fig. 7 and other telescopic views show the E rim illuminated and indicates a complex system of ridges similar to the inner slopes of Alphonsus. The mean slope angle of the inner rim section from 9°26′30″ W, 42°52′ S to 9°30′ W, 42°55′ S is about 22°. The steepest slope noted in the inner area is about 36° over a lateral distance of 120 meters (Fig. 11). No detailing is possible here, but the part of Tycho's inner rim shown on *Orbiter V* shows lakes and ridges, as on the outer slope.

The Tycho rim is not an edge or ridge, but a plateau that on its eastern side is dotted with lakes, often connected by small flows (Figs. 12 and 13).

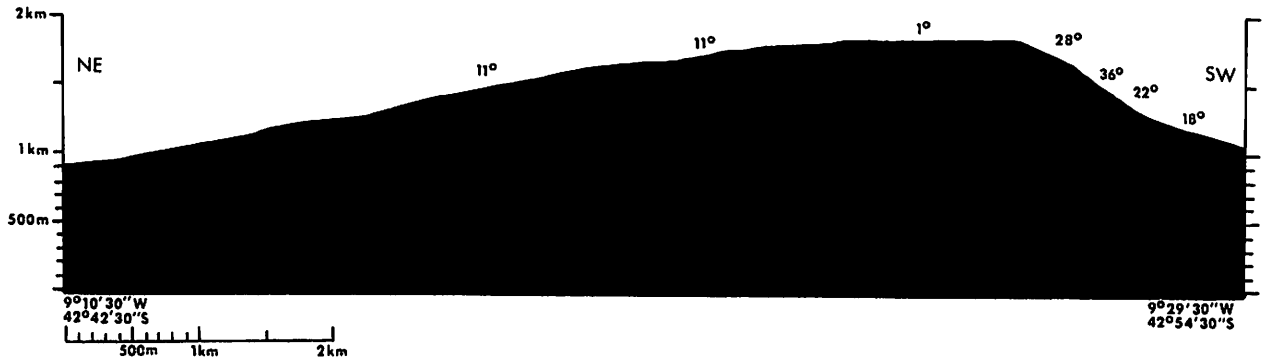

Fig. 11 Cross section of Tycho's rim, with measures of slope angles.

Fig. 14 illustrates a terrestrial area showing flows similar to those observed near Tycho.

Full-moon records (Fig. 1) indicate that dark rim material extends outward downslope and covers the central parts of the area modeled. In analogy with the flows shown in Fig. 14, it may be assumed that these central parts have received dark deposits from elevated sources. The central lake region is cut off on the S by an unusual widening of the Tycho rim (Fig. 12). This rough terrain S of 42° 55′ S contains even more lakes than the modeled area and is more elevated, and may be a source of lava for the modeled area.

The relative elevations of the lakes are of great interest in their interpretation and may be found stereoscopically (Fig. 15). Most lakes appear quite level, though not always smooth. Fig. 16 shows numbered designations for 25 lakes. Additional lakes were identified later but the original numbering was retained, with additional lakes designated with a double number (indicating location between neighbors). With possibly one exception (the westward extension of L8), *the lakes are dark in tone,* and they are clearly of different texture from their surroundings though they show some terraces, hills, craters, and rocks.

b. The lake levels derived, based on shadow measurements, stereo viewing (Fig. 15), and elevational experimentation in the model, are found in Table I.

It is seen that the northward tongue of L8 overlaps the shore as a "meniscus", *level on top but curved downward at the edge.* Lesser meniscus edges are found on L9, L13, L20, L5, L19, and L21. Often there is at least a sharp demarcation between the lake and its surroundings. Such a lip is typically less than 5 m high, often much less. However, on L8 the lip approaches 10 m, sufficient to show in cross sections of the area (Fig. 17). NW of L8 and seemingly entering its W extension, a flow-like feature extends from the N, starting possibly as far N as a lake between L2 and L5, designated as L2-5, which itself contains a peculiar rift. The feature NW of L8 is not level or flat, yet resembles a lava flow.

Other level places may contain dark lake material, e.g., L9-11 (Figs. 15, 16), and L17-23, associated with the broken craters interrupting the slope between L19 and L17; also a series terminating N and E from L19, N from L14 to L8, and between L24 and L20.

The stereo pairs and Table I show that there are four *main groups of lake elevations:*

1. The high Tycho rim: L12, 17, and 18.
2. The upper slopes: L5, 7, 10, 23, 24, and 25.
3. The central region: L1, 2, 6, 8, 9, 13, 14, 15, 19, 20, 21, and 22.
4. The lower plain: L3, 4, 11, and 16.

At two locations the lake levels fall abruptly: from L15 to L14, and from L12 to L17. These breaks are interpreted as *normal faults* (Fig. 18,

TABLE I

FEATURE L#	ELEVATION *	FEATURE L#	ELEVATION *
12	2000-2020	15	680-700
18	1730	14	660-680
17	1680-1660	9	620-660
5	1380	6	520-540
23	1210	8	520-540
7	1180-1200	22	500
19	900-920	2	440-460
10	880-920	16	440
24	850-860	3	360
25	820-840	1	340-360
13	720-740	4	120
21	750-760	11	80-100
20	730-750		

* In Meters above Reference Level, 42°27′ S, 8°30′ W.

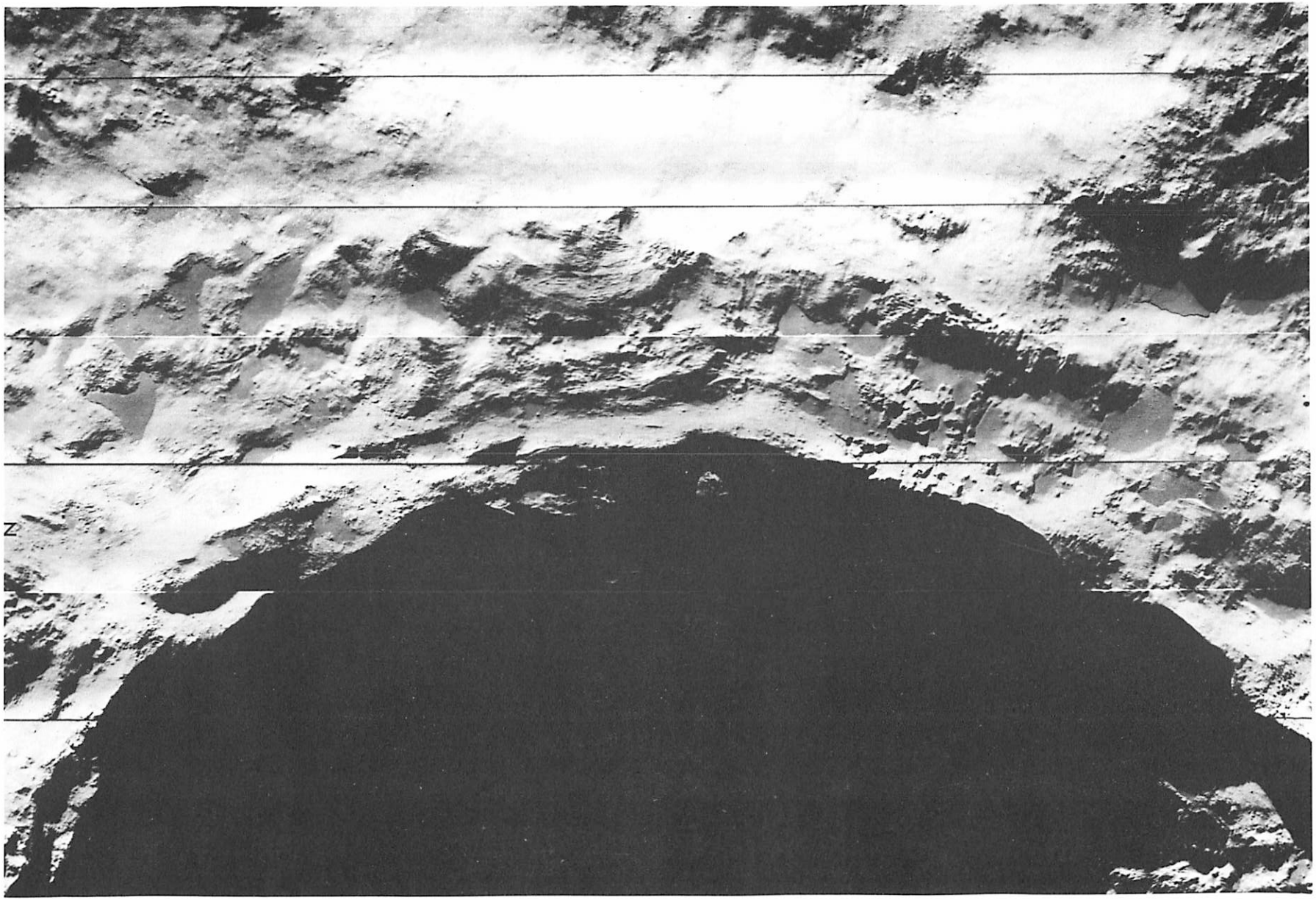

Fig. 12 *Orbiter V* M 127, showing lakes in model area and beyond, N left.

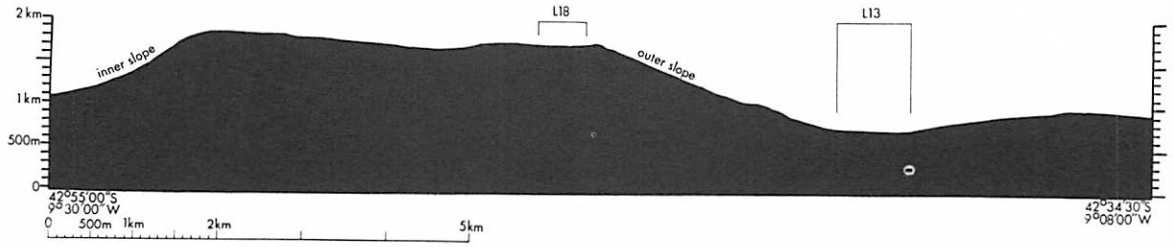

Fig. 13 Cross section of the rim of Tycho through left (N) part of Fig. 12, based on model, cf. Fig. 16 for numbers.

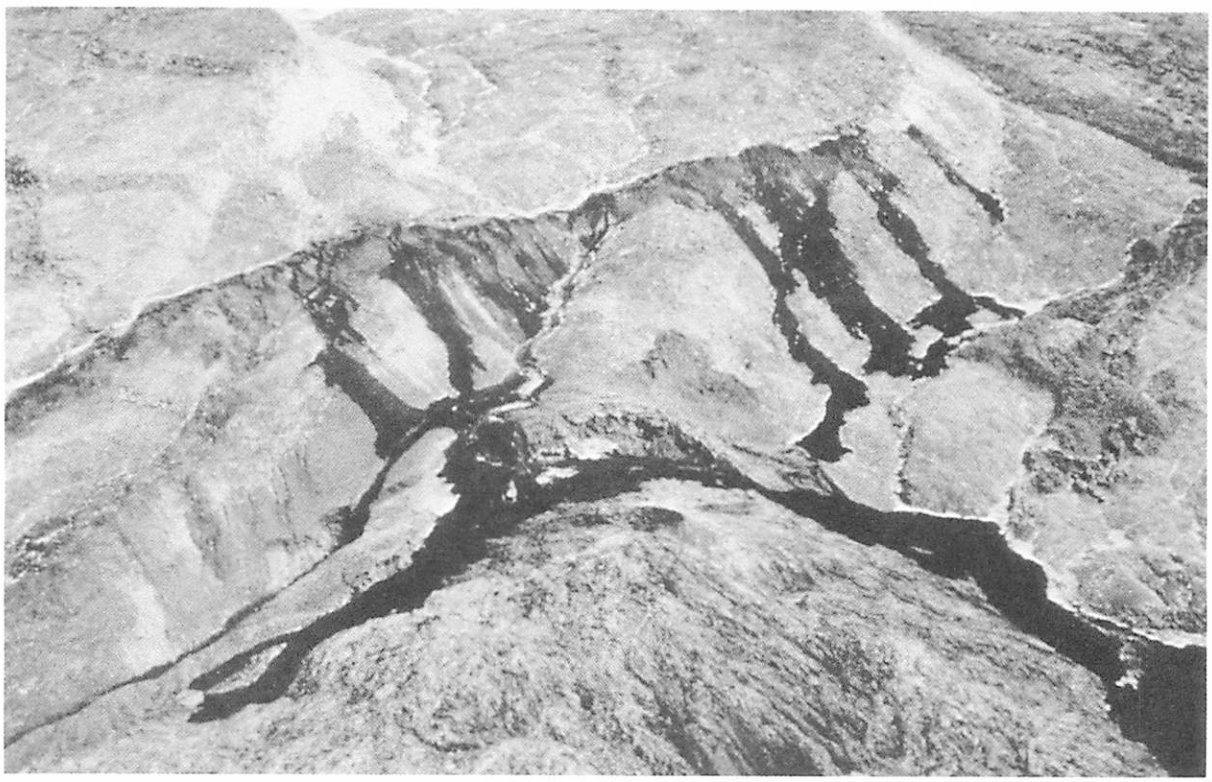

Fig. 14 Ribbons of basalt in Erta' Ale Mountains from "The Afar Triangle" by Haroun Tazieff in *Scientific American*, Feb. 1970 (courtesy Dr. Tazieff).

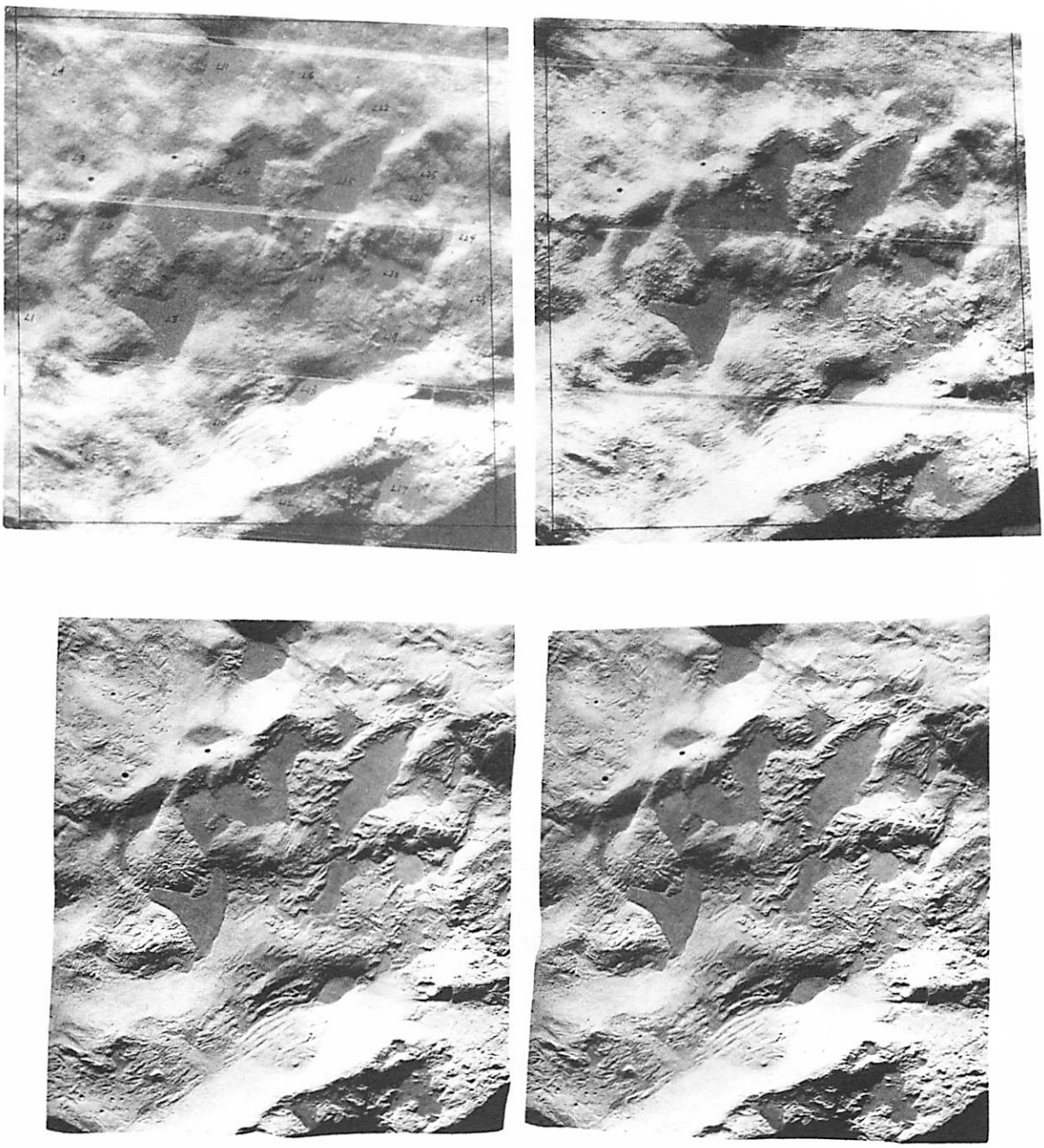

Fig. 15 *Orbiter V* M 125 and M 128, stereo pair *(above);* compared with stereo pair of Relief Model *(below).* N to the left.

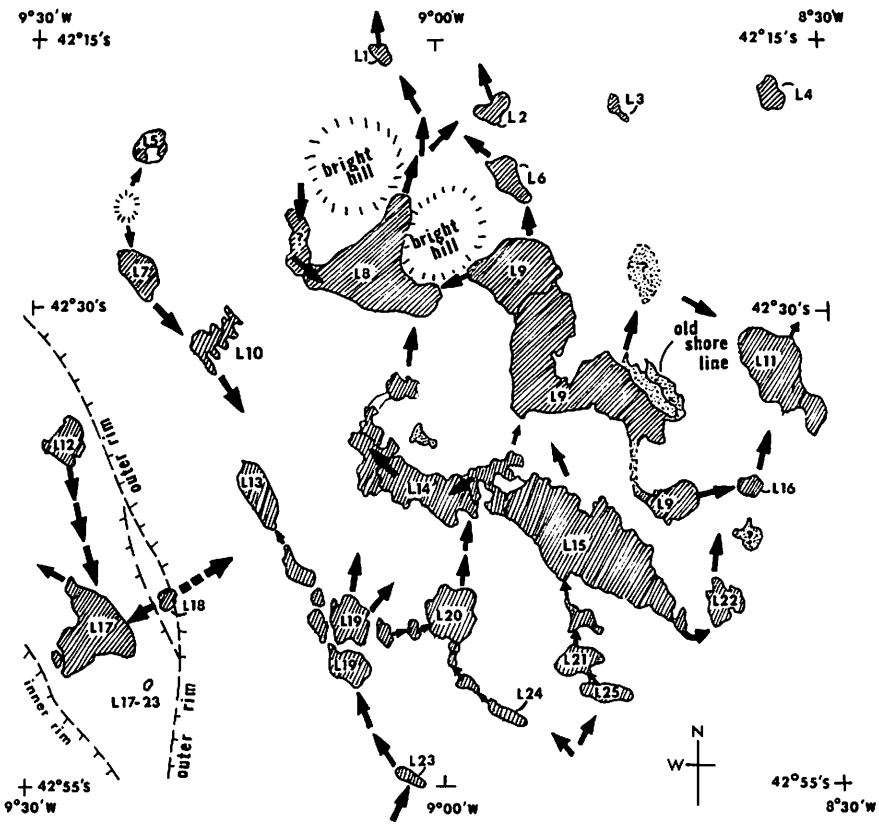

Fig. 16 Outlines of lakes and flow directions, inferred from *Orbiter* stereo data used in Model.

which shows the minimal slopes consistent with the data).

Figs. 19 and 20 clarify the stepwise level difference between L12 and L17 on the rim of the model (cf. Figs. 2 and 3). A *series of falls* is present between these lakes, and L17 appears to have flowed down onto the inner slope of Tycho (in shadow) (Fig. 19).

c. Connections between lakes; sources of lake material — The often-small elevation differences between the lakes, and their connections through visible flows, indicate a *pattern of movement*. All V-shaped valleys appear to contain one or more lakes, often connected by streams. *L12 is the highest lake,* with its source not obvious (possibly *internal* or an adjacent feature to the E). There is what could be a cinder peak directly to the S of it. Once L12 was filled, its material appears to have flowed downward, S to L17 and possibly also W, to the interior of Tycho. L18 is isolated, higher than L17, and its material could not have come from L12. There is a complicated set of features to the W and S of it. A ridge with a cleavage (cf. Figs. 2 and 3) lies directly between L17 and L18, about 100 m higher than L17 and 60 m higher than L18. Conceivably it could have been a source for both (Fig. 16). L23, 1210 m high, lies N and downhill from a region of extensive lakes (outside the model; cf. Fig. 12). In stereo, L23 is seen to lie above L19, into which it may have flowed, while L19 itself is the highest of a series of terraces leading into L13, L10 and L14, probably all due to flows. This flow process appears to continue from L14 to L8. This progression from L23 to L8 is nearly the full N-S extent of the model (Fig. 2, 3, and 16).

The large lake lying S of and above L23, and outside the model (cf. Fig. 12), could easily have been the source of both L24 and L23; however, a broken crater lies above and between them also, and could be a source as well. There may be a connection between L24 and L20 and an extension into L14. In its circular shape, L20 resembles an old crater.

Once material can be accounted for in L25, its movement to L21 and L15 is easily traced. From L15 material could go to L22 and less definitely to

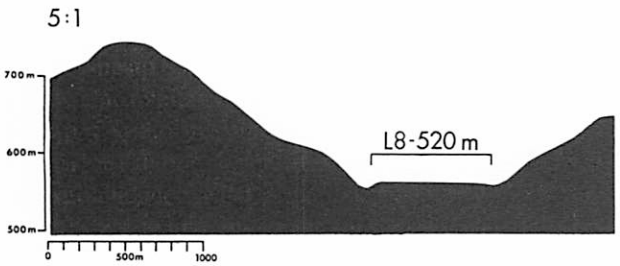

Fig. 17 Cross sections of L8 tongue, with 5:1 vertical exaggeration.

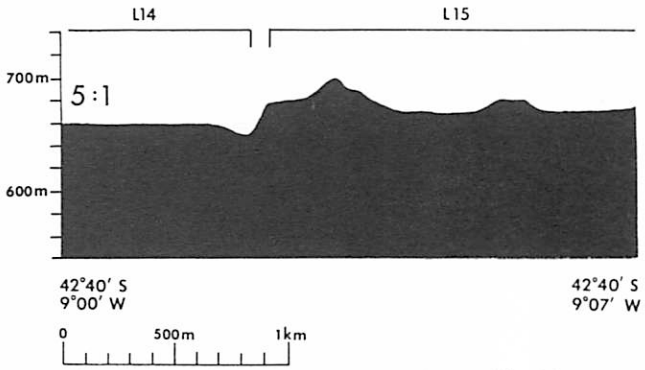

Fig. 18 Cross sections of L15 and L14 drop, with 5:1 vertical exaggeration.

L9. Connections between L9 and L16, L9 and L6 are uncertain. Connection between L16 and L11 is complex but not difficult to follow. Connection from L6 to L2 and the small lakes to the N of the model is definite. No connections involving the isolated lakes L3, L4, L5, L7 and L10 were seen or expected from the types of terrain separating them.

The level of L9 shows some indication of once having been higher than it is now; because eastward of its shores appear dark areas of higher elevation, on terraces and slopes tilted westward. (Alternatively, these ridges could have been first exposed to lavas and then uplifted).

Several mounds with cleavages at their summits are evident near L5, L7 and L10. One, near 42°24′ S, 9°23′ W is especially dramatic under low sun (Figs. 2, 3, 15). It rises to higher than 75 m, with dimensions 250 × 550 m (cross section in Fig. 21). These mounds may be sources of some lake material.

The linear connections found between several lakes seem to be part of an overall lineament system (Fig. 28), and are not *formed* by flows. They are *used* by the flows, as is most clearly seen in the NW corner of the model. At the S end of this system, and nearly at right angles to it, is another set of linear features connecting L19 and L20. With highly fluid lavas, only a limited number of sources need be assumed.

The "craters" on the SE slope, some 600 × 800 m in size, are strongly breached downhill to the N and appear to contain some lavas. Creases can be traced from these depressions to L19 and L13 (see Fig. 15). All of the above discussion is *summarized by assuming a series of sources on the rim, near the outside crest, flowing downhill, transforming what was once a series of roughly concentric ridges into terraces.*

The dark Tycho lakes have counterparts else-

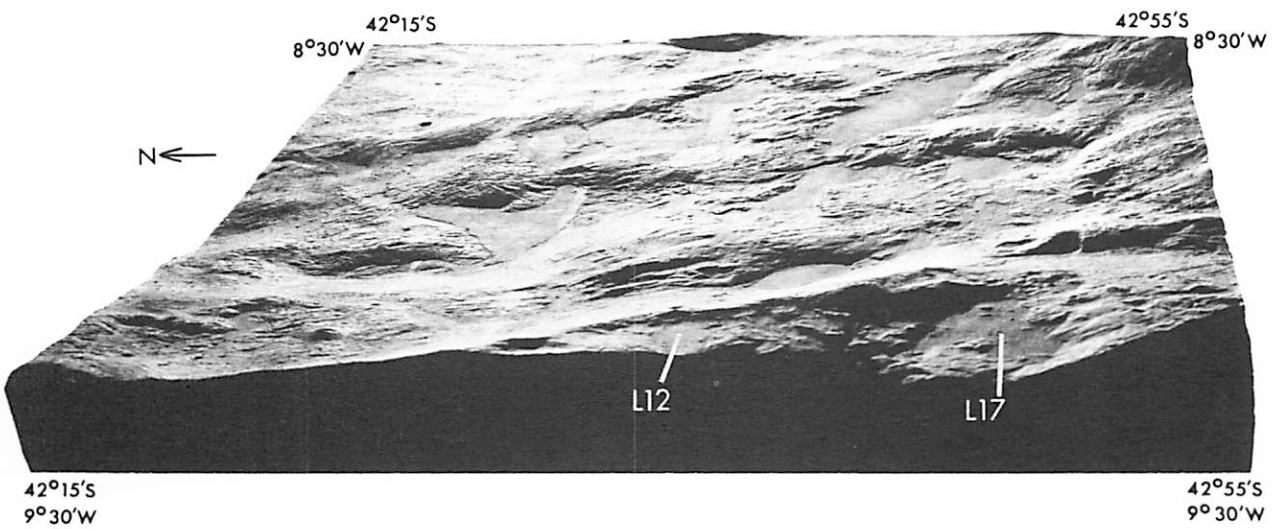

Fig. 19 Oblique view of the model: Looking east with lighting simulating *Orbiter V* illumination conditions. (⊙altitude 11°, ⊙azimuth 12° N of E).

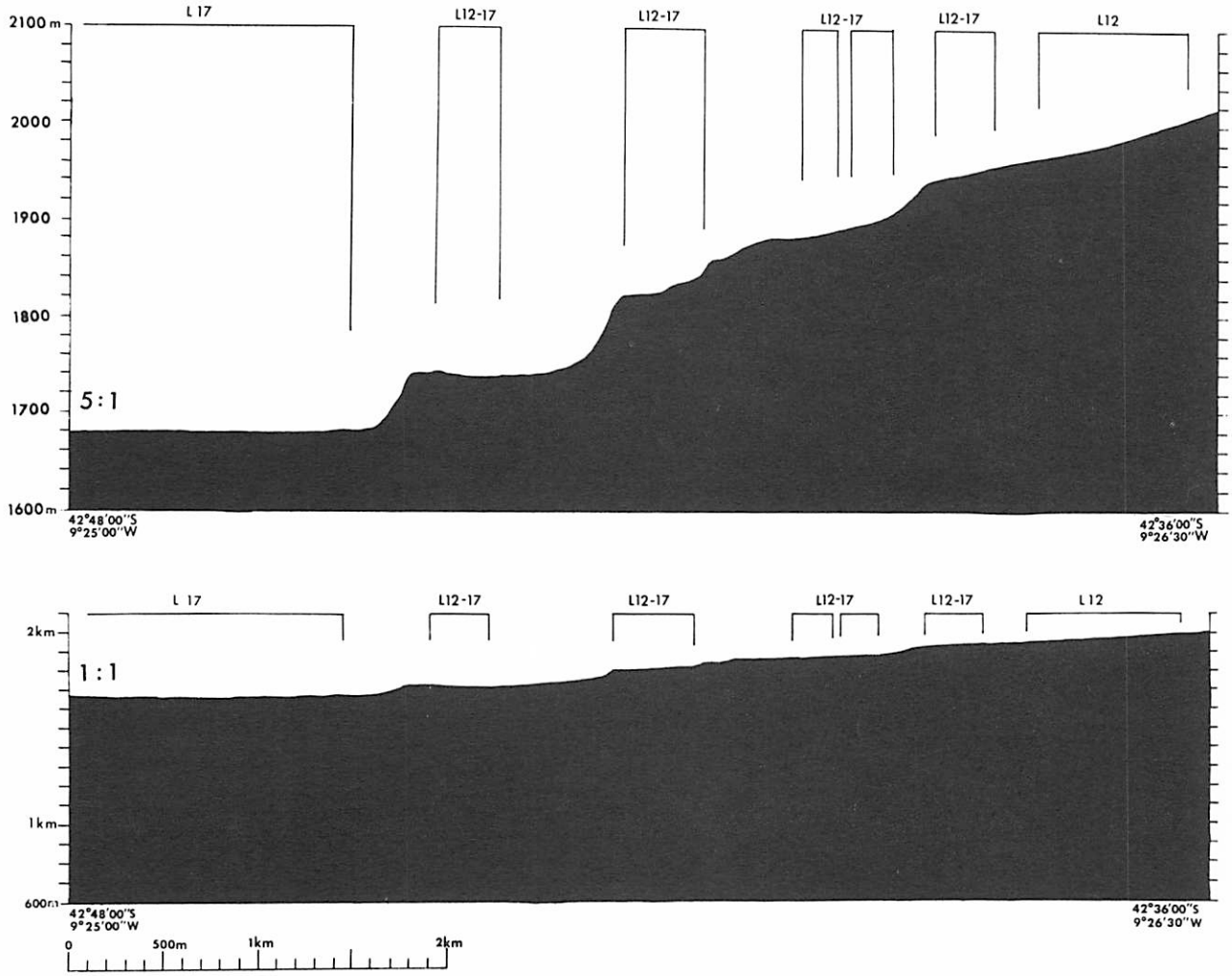

Fig. 20 Cross sections of L12 to L17 drop, with 5:1 and 1:1 vertical exaggeration.

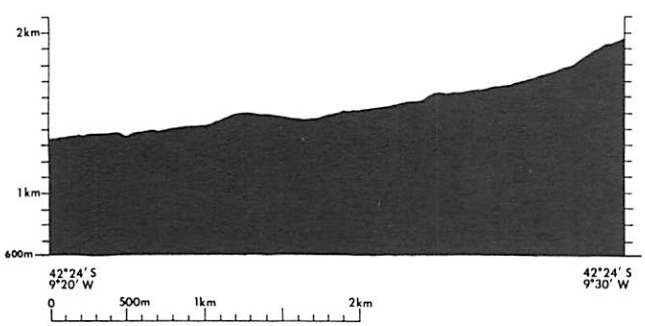

Fig. 21 A prominent positive feature near L5 and L7, 1:1 cross section.

where on the moon. Tsiolkovsky on the far side (cf. Fig. 22), approximately three times the diameter of Tycho, exhibits the same kind of darkish, level areas on its outer slopes.

The NE rim of Alphonsus, modeled in 1966–68, contains at least one lake resembling L13 of Tycho. Although the Alphonsus lake is on the inner slope and contains many craters and collapse depressions, its boundaries are also defined by surrounding ridges (JPL-NASA *Ranger IX* Report).

High-resolution *Orbiter* photos are available of the region NW of the present model area which contains some small dark lakes. Sections of the high-resolution records are reproduced in *LPL Comm.* No. 150 (Figs. 8, 9). It is seen that these smaller lakes possess a polygonal pattern of tilted plates and cracks, with some craters and small rocks. Some larger rocks are evident on most of the lakes in the model area; whereas cracks up to 5-m wide and numerous smaller rocks are suspected. By analogy, some of the apparent terracing could be platelets and cracks in the surface. The largest lakes actually seem the smoothest.

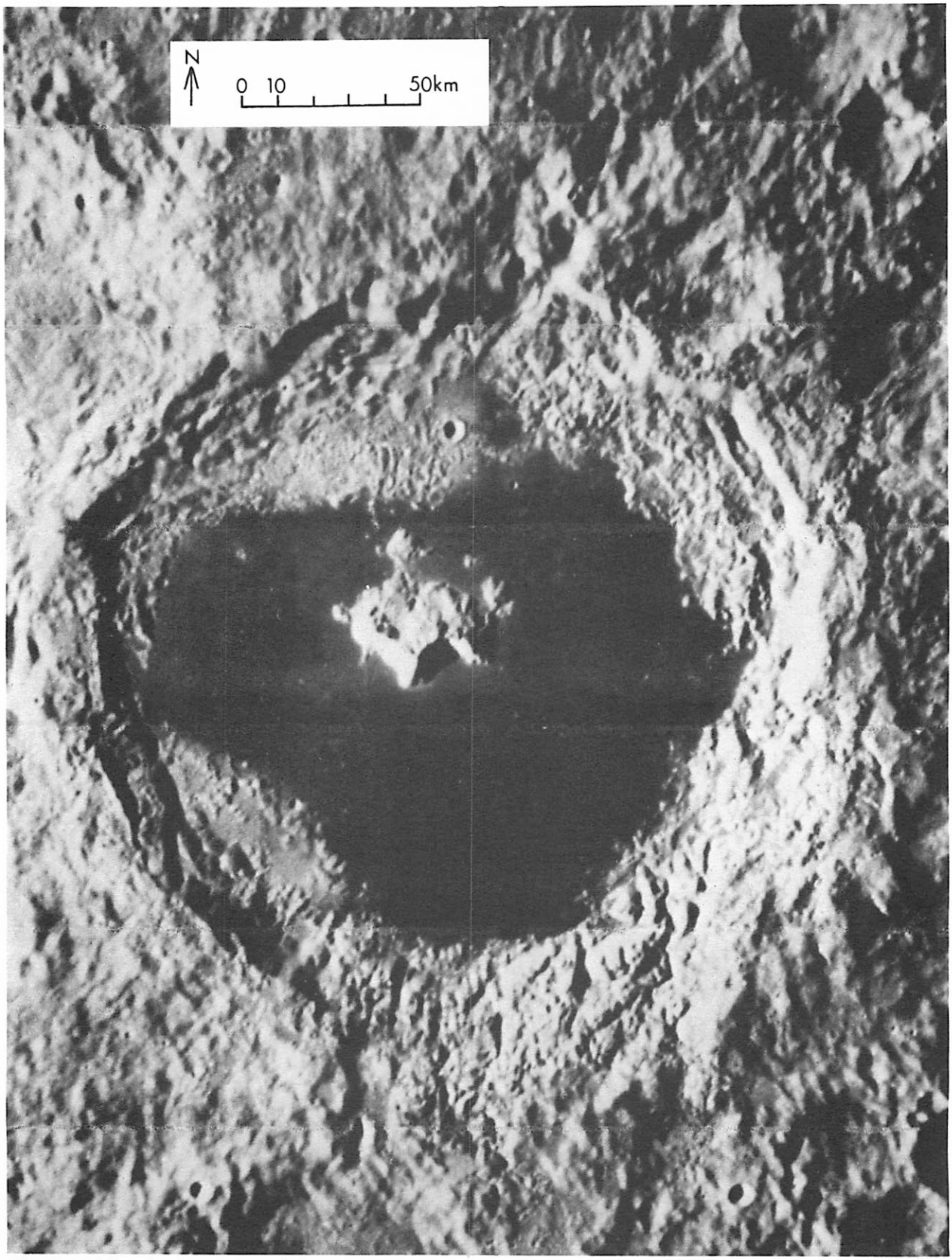

Fig. 22 Tsiolkovsky Crater, from *Orbiter III* M121; note numerous lakes on outer ramparts. (Boundary lines between strips retouched).

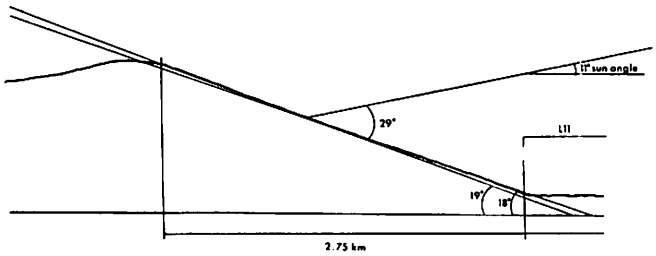

Fig. 23 Cross section, illustrating solar illumination on slope facing sun.

d. Slopes — Although Plate C483 yielded an *inner* slope of Tycho somewhat greater than 36° (Fig. 11) and 35 mm photos (Roll 8, #21) taken June 28, 1969, indicated 39°, visual observation on several nights has indicated that the slope does not exceed 36° and this is accepted. Within this slope no detail can be found from available records, except that there is a ridge at the foot, some 760 m below the inner crest. This is still higher than L13 and L19 at the foot of the outer slope.

The *outer* slope in the model area is about 2.8 km wide and drops 1.1 km, an average slope of 20°. The detail is mostly burnt out in the photographs but some texture is shown. The solar altitude for the *Orbiter V* frames was only 11°1, but with a slope of 18-19°; the effective illumination angle is near 29° (Fig. 23). In addition, it appears from full-moon records that the slope consists of brighter material.

Just N of L13 is a major slump block; at its base a fold connects L10 to L13.

Although the drop from the Tycho rim to the lake region is the largest, there is a further drop 1.3 km further east, starting with a low ridge. In low-resolution photographs this ridge appears as the rim of a shallow crater, 28 km in diameter (Fig. 7, NE of *B*). Between L9 and L11 this rim slopes 14° outward (Fig. 24), but much less along most of its length. On the north, the slope is only a few degrees, 2° to 6° between L6 and L4 (Fig. 25). South of L22 the ridge disappears. The shallow crater referred to contains isolated shallow lakes. There is some indication that its rim has a higher albedo than the central lake region but is not as bright as Tycho's rim or the two bright hills (Figs. 1, 6).

The slopes in the vicinity of L24 and L25 are somewhat uncertain on the model. In stereo their steepness is not as great as the photometric effects

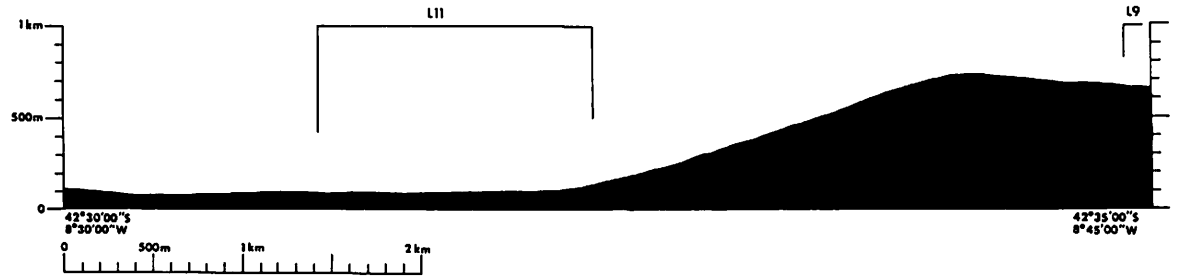

Fig. 24 Cross section of slope west of L11.

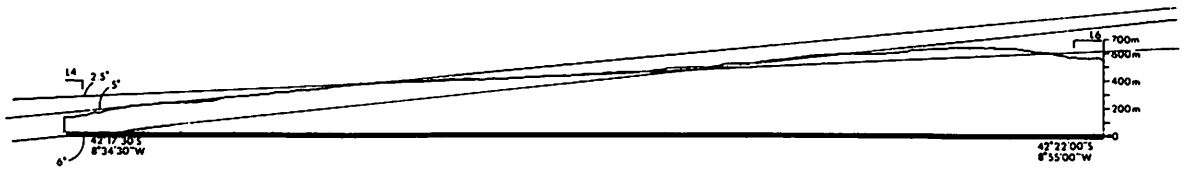

Fig. 25 Cross section of slopes between L6 and L4.

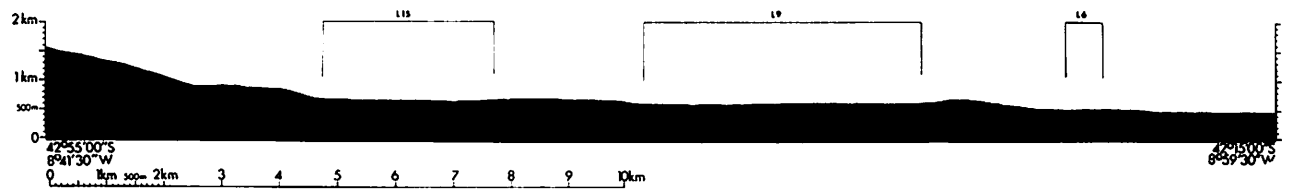

Fig. 26 Diagonal cross section of model, showing steepest slopes on S end.

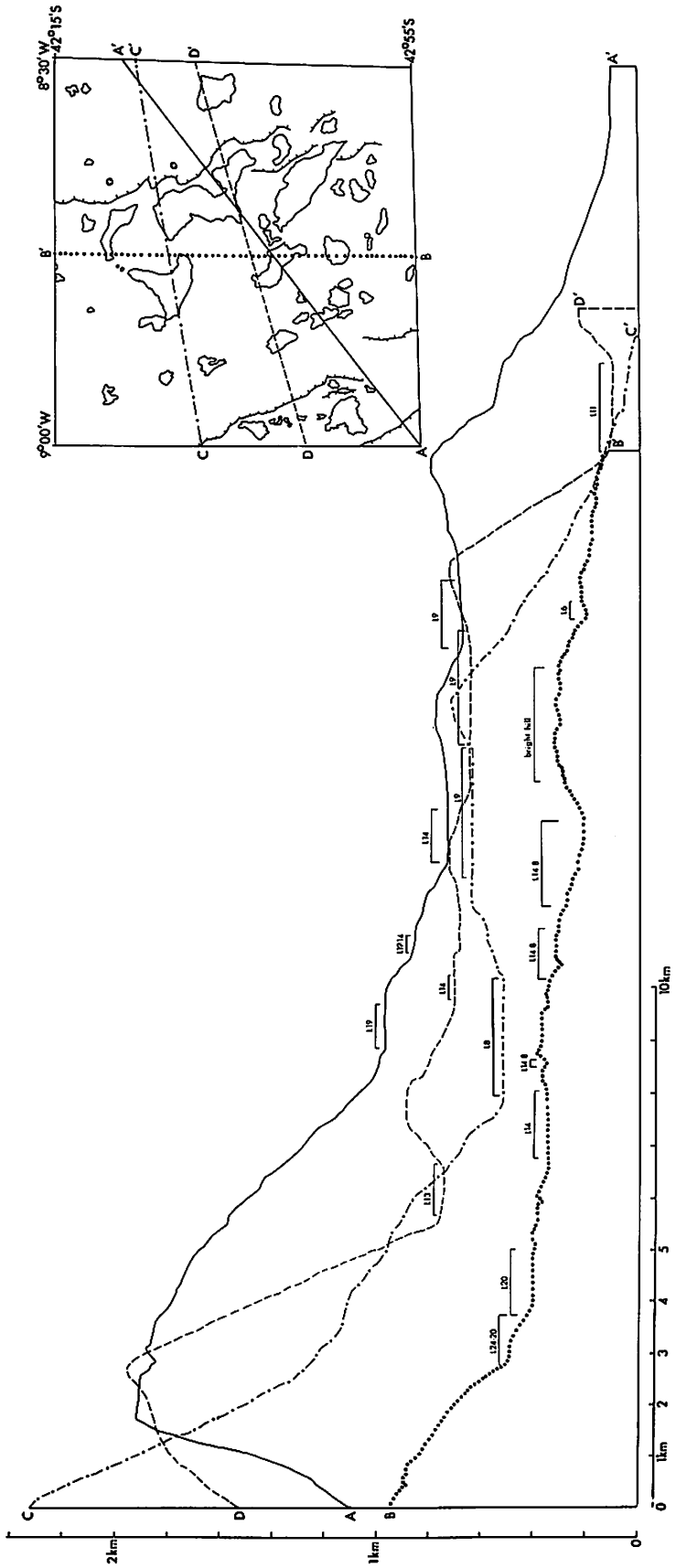

Fig. 27 Cross sections (A, B, C, D) of model, with 5:1 vertical exaggeration.

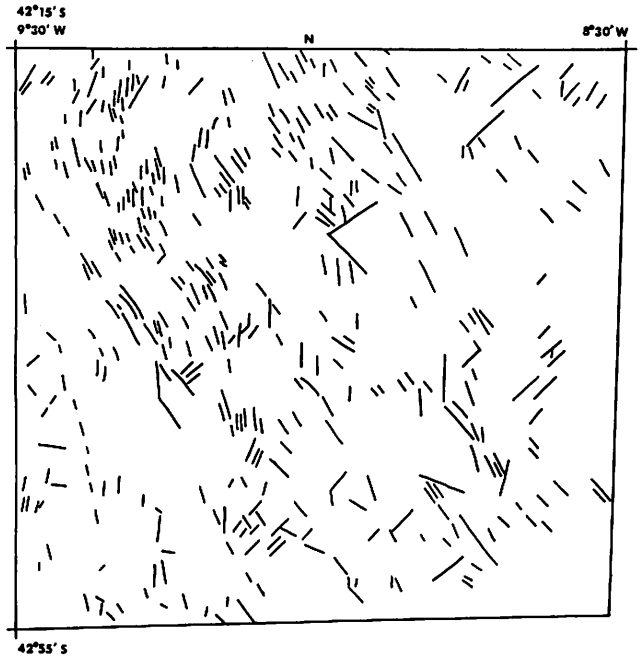

Fig. 28 Linear trends in the model area.

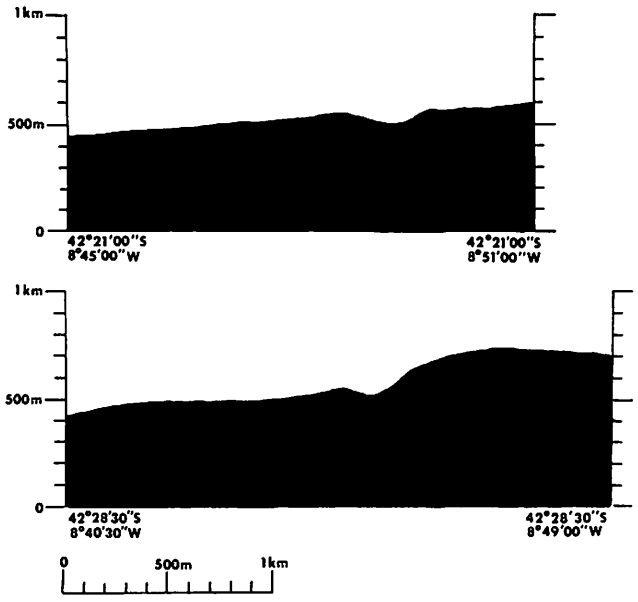

Fig. 29 Cross sections of two sharp craters E of L9 and L6.

would indicate. Along 9° W we find slopes up to 18° for a distance of 600 m and of 16° for 2 km (Figs. 26, 27B). Other examples may be read from Fig. 27A-D.

On the bright hill, N of L8 (Fig. 16), the slopes are 11°-27° for distances of 100-700 m. A prominent drop from L15 to L14 which covers 120 m has a slope of 12° or greater (Fig. 18). On the other hand, the longer drop from L9 to L8 is at grazing incidence and is well determined at 8°-9°. In both cases, the slopes are westward, *toward* Tycho's rim, a reversal of the general slope. The two reverse slopes are both NS, nearly aligned, crossing the center of the model. The full extent of these NS lineaments is best seen from the Relief Contour *Map B*.

It is not easy to determine the slopes of the isolated blocks, but there are indications that some may be cliff-like. Blocks 25-200 m across appear throughout the area. They are especially abundant on the Tycho rim, including some protruding through the lakes. Another grouping of these large blocks or rough broken ridges occurs on the two bright hills, especially the Eastern one. All these protrusions are usually limited to about 10 m height.

To *summarize,* the slope angles in the region of the model range from 0° for the lakes to about 36° for the inner slope of Tycho. Some small features may have steeper slopes. As elsewhere on the moon, slopes around 12° are common. Compared with slopes on Alphonsus and in Mare Cognitum, the outer ramparts of Tycho are rough at several scales, yet possess many near-level features also. Compared to volcanic features in Hawaii and Oregon, the slopes of Tycho are quite steep.

e. Linear trends — Throughout the area modeled, linear ridges and rims trend predominantly about N 30° W, with a smaller group trending nearly at right angles, N 50° E. In addition to this, some trend about N 3° E. The results are plotted in Fig. 28, compiled with the assistance of Mr. R. Strom. Some of the lineaments in Fig. 28 correspond to lake boundaries, such as L9, L13, L21 and L25 (cf. Fig. 15). Part of the Tycho rim itself fits into this pattern. The direction N 38° W corresponds to several lake boundaries and ridge structures. Subtle, softened linear trends (at N 50° E) are found in the shallow "crater" between L9 and L4 (Fig. 2). These lineaments become stronger in the higher country near L25, L21, and L22. The N-S trends are least conspicuous on the original photographs (Fig. 2) but in the Relief Contour *Map B* long linear trends in the N-S direction are evident. The three major trends found here agree with those of the larger features discussed by Strom (1964).

f. Craters — On the outer ramparts of Tycho, only a few craters occur. These are sharp and presumably due to genuine impacts. In addition, there are irregular depressions which are usually breached and presumably volcanic; particularly south of L17 there are several such features in rough terrain (Figs. 16, 15, and 2).

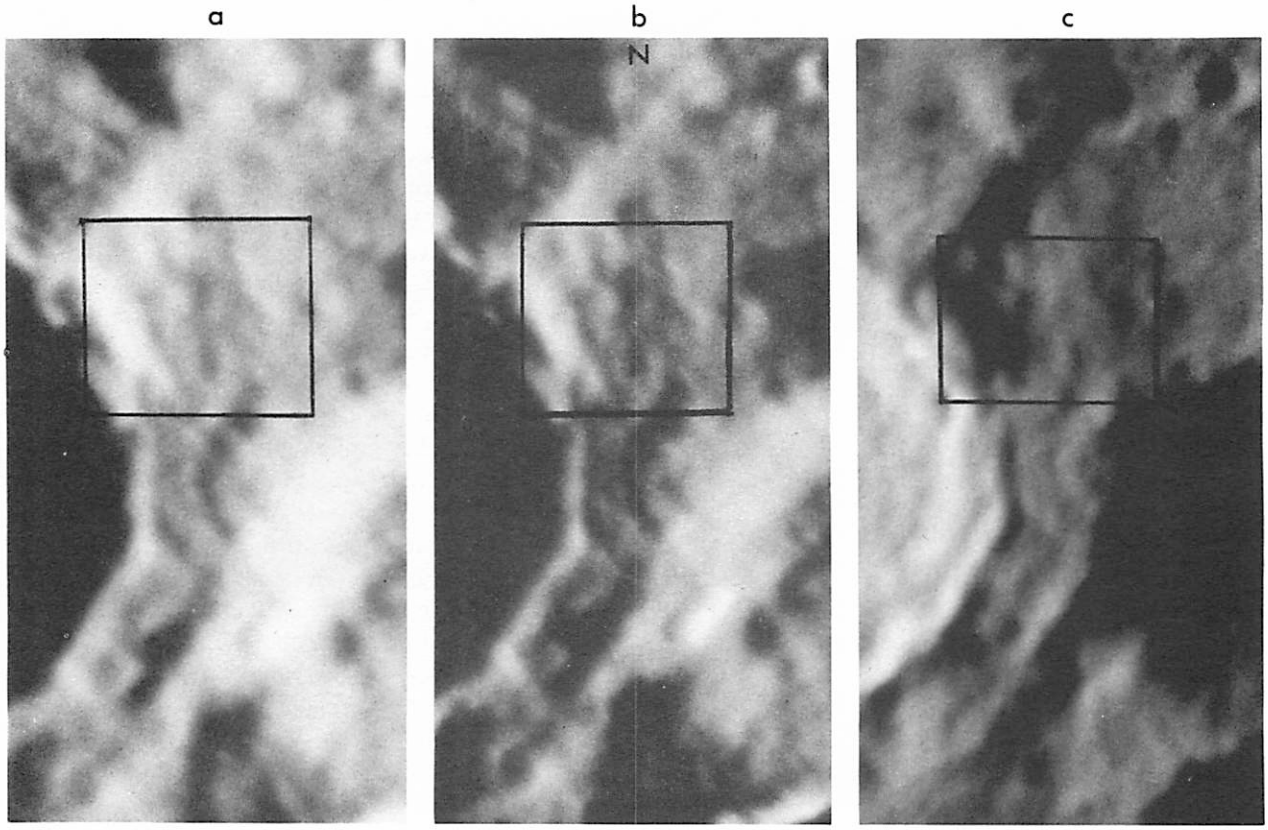

Fig. 30 Three 61-inch photographs of E rim of Tycho: (a) C838, ⊙ altitude 6°.2, ⊙ azimuth 4° N of E; (b) C4114, ⊙ altitude 3°.3, ⊙ azimuth 1° N of E; (c) C2435, ⊙altitude 10°.7, ⊙ azimuth 12° N of W. See Fig. 31*a*, *b* and *c* for comparison with Relief Model.

Fig. 31(a) ⊙ altitude 6°.2, ⊙ azimuth 4° N of E.Relief model under illumination matching Fig. 30(a).

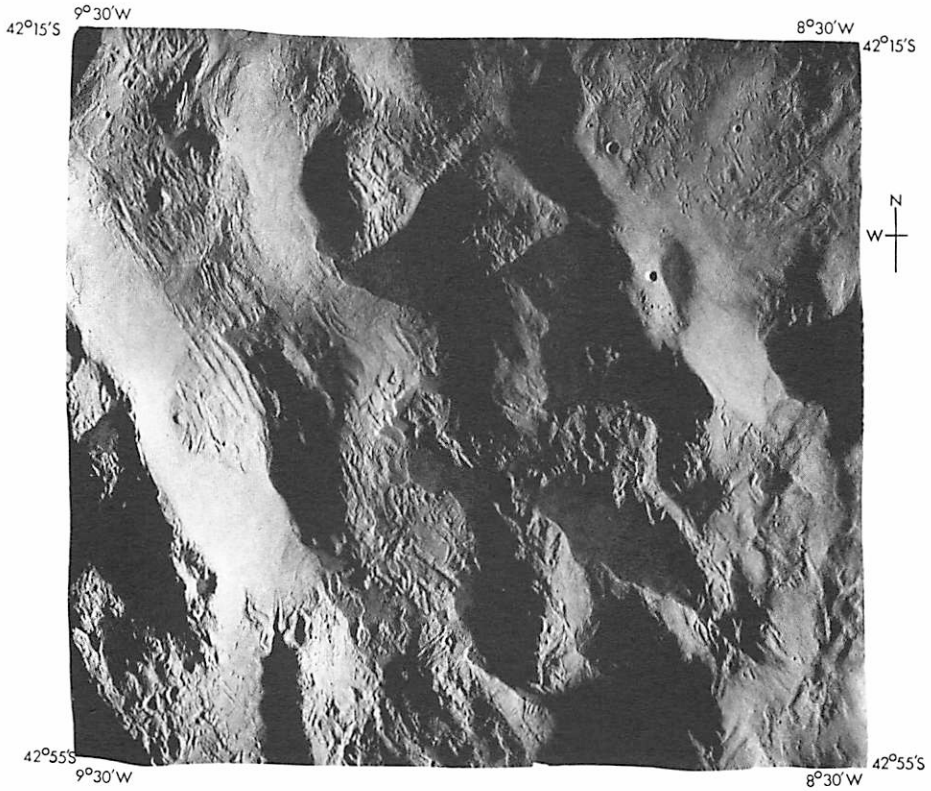

Fig. 31(b) ⊙altitude 3°3, ⊙azimuth 1° N of E. Relief model under illumination matching Fig. 30(b).

Fig. 31(c) ⊙ altitude 10°7, ⊙ azimuth 12° N of W. Relief model under illumination matching Fig. 30(c).

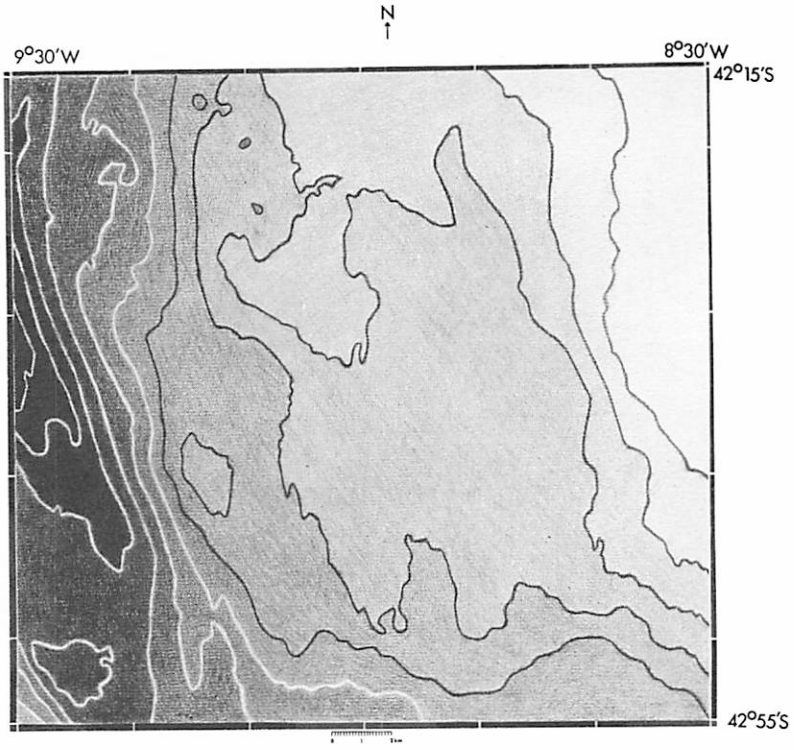

Fig. 32 Contour map of model area, based on *Map A*, interval 200 meters.

There are many small pits throughout the model area, but on the lakes there are few craters. Two sharp craters, one between the north end of L9 and L11, and one between L6 and L3 are approximately 350 m in diameter and 65 m in depth (Fig. 29). They have slightly-raised rims (a few meters). One lies on a slope. Perhaps these two craters contribute to the slightly higher albedo of the rim E of L6 and L9.

Somewhat more craters appear to occur on the undulating surface between L6 and L4, and on a relatively level area at the intersection of Tycho's rim and the ridge in the NW corner of the model.

C. Wood and W. Hartmann have made a crater count of the region (see Appendix II). The location of larger craters can be found on the topographic maps.

g. Positive features — The positive features in the area are of interest because their outlines tend to become less defined with time, whereas depressions keep a certain sharpness even when partly filled. This trend is less true in a region of lava flows, where an old shoreline may be found at a higher level. Only a few examples of positive features are described here. Many may be seen by inspection of the records reproduced.

Between L17 and L18 a narrow ridge is seen that reaches nearly the highest level on the model. A source of lava-like material may be located here and could account for L18. There are many isolated positive features near this ridge and in L12 and L18.

The rocks or hills that appear as islands in L17 may be higher in albedo than L17 itself, possibly indicating greater age. Many 'islands' seem to be continuous with nearby arcs or linear trends, indicating once again the relative freshness of the lakes.

The extreme roughness of the two bright hills and the Tycho rim (except for the lakes) is exceptional and is not matched by other convex features, such as those between L15 and L9, or L13 and L15, or especially the complicated but smoother basin E of L6. This rough terrain is definitely not a concentration of craters.

h. Albedo differences related to relief — As commented before, albedo differences become greatest at small phase angles. Since relief is normally modeled from photographs with large phase angles, albedo differences are incidental. However, the albedos of most small lunar areas are not known. Consequently, an effort was made to correlate bright areas with relief features and use the results on the model.

The dark Tycho halo seen in Fig. 1 cannot be

fully explained by dark flow material although lakes occur throughout the halo. On the best full-moon records there is differentiation within the halo. If it is assumed that the lakes occur in the darkest patches, a fair correspondence is found. If the dark material had filled all enclosed basins and left a dark coating this would explain the pattern noted in Fig. 2, where it appears that material has flowed from L17 and L18, on the rim, to L15 below. It also suggests a coating over most of the center area, between L9 and L13, L14, and L8 (Fig. 16).

The highest albedos show correspondence with relief features. Two bright spots shown on full-moon records were identified with two broad hills on the N end of the model. These rocky hills are separated by L8.

The rim of Tycho, including the plateau containing L12, L17, and L18, is bright except for some dark breaks presumably corresponding to lakes.

An arc corresponding to the rim E of L9 and L6 shows up slightly bright. This is one of the features identified by Fielder (1965). He states: "Pairs of plateaus occur . . . One appears to have been filled by a flow of blocky lava from the western (eastern) ringwall graben of Tycho."

Generally, the dark areas extend beyond the lakes which indicates movement of the dark material. Therefore, most of the lakes in this region resulted from younger material flowing over older terrain.

i. Tycho's rays — There is no correspondence between Tycho's rays and features in the model area. The rays seem to have been formed beyond the halo. The high ridge that lies N of the model area, radial to Tycho, is not a bright feature such as Tycho's rim. While the two bright hills in the model area lie at the foot of this ridge, they differ in albedo so much that the ridge is nearly invisible at full moon.

j. Comparison of model with earth-based photographs — Supplementing the comparisons with *Orbiter* records made in Figs. 2 and 3 and elsewhere in the text, we reproduce here comparisons with three selected telescopic photographs representing different phase angles.

Figs. 30*a*, *b*, and *c*, show the east rim of Tycho (with the 61-inch telescope) under illuminations listed in the legend. We have duplicated these illuminations on the model photographs, shown in Fig. 31*a*, *b*, and *c*. While the correspondence is within the resolution, the urgent need of high-resolution coverage with near-sunset illuminations is apparent.

The gross features of the region are shown once more in the contour map, Fig. 32, with interval 200 meters, based on the topographic *Map A* which has 20-meter contour intervals.

5. *Conclusions*

Although the Tycho lakes appear to be similar to maria and flooded craters, there are differences. They contain few craters and are more nearly level and are probably *much younger*. The integration of data attempted here has probably gained the maximum amount of information from the available records. Higher resolution photography would refine information on the flow edges, crater characteristics, and lake textures. A manned landing would make possible closer comparison with the maria and especially allow a radio-isotope *dating of the Tycho lakes.* The several closely-spaced large, level lakes, among otherwise steep and rough terrain, would be *favorable landing sites,* and they will be adjacent to very interesting highland areas.

Acknowledgments. I wish to extend thanks to Dr. G. P. Kuiper for introducing a professional sculptor to the moon, and for his general support; and to Messrs. Whitaker and Strom for their professional assistance and criticism. Mr. S. Larson aided the program with numerous photographs. Mr. F. de Wiess assisted with the development of special instruments; Mr. D. Harris with some of the computation. Mrs. B. Vigil assisted with the preparations of the text, the cross section, and especially the maps. The final cast of the text was composed in consultation with Dr. Kuiper. The project was supported by NASA NGR-03-002-191.

REFERENCES

Aeronautical Chart and Information Center. 1967, "Tycho," USAF Lunar Chart LAC 112.

Fielder, G. 1961, "On the Origin of Lunar Rays," *Ap. J.*, 134, 425–434.

Fielder, G. 1965, *Lunar Geology* (London: Lutterworth Press), pp. 62–63.

Kuiper, G. P. 1965a, "Interpretation of *Ranger VII* Records" in *Ranger VII. Part II. Experimenters' Analysis and Interpretations,* JPL TR 32–700, p. 60.

Kuiper, G. P. 1965b, "Lunar Results from *Rangers 7* to *9*," *Sky and Telescope,* **XXIV**, No. 5, pp. 298–308.

Kuiper, G. P. 1966, "Interpretation of *Ranger VII* Records," *LPL Comm.* No. 58, 4, 52.

Kuiper, G. P., Strom, R. G., and LePoole, R. S. 1966, "Interpretation of the *Ranger* Records" in

Ranger VIII and IX. Part II. Experimenters' Analysis and Interpretations, JPL TR 32-800, pp. 120–121, 123–129.

Lunar Sample Preliminary Examination Team. 1970, "A Preliminary Examination of Lunar Samples from *Apollo 12*," *Science,* **167**, 1325.

Moore, J. G. and Peck, D. L. 1965, "Bathymetric, Topographic, and Structural Map of the South Central Flank of Kilauea Volcano, Hawaii" (Washington: U.S. Geological Survey), Misc. Geologic Investigations Map I-456.

Oetking, P. 1966, "Photometric Studies of Diffusely Reflecting Surfaces with Applications to the Brightness of the Moon," *JGR,* **71**, 2505–2513.

Saari, J. M. and Shorthill, R. W. 1966, "Hot Spots on the Moon," *Sky and Telescope,* **XXXI**, No. 6, pp. 327–331.

Shorthill, R. W. and Saari, J. M. 1965, "Nonuniform Cooling of the Eclipsed Moon: A Listing of Thirty Prominent Anomalies," *Science,* **150**, 210–212.

Spurr, J. E. 1945, *Features of the Moon* in *Geology Applied in Selenology,* **II** (Lancaster, Pa.: Science Press), pp. 106–108.

Stearns, H. T. 1966, *Geology of the State of Hawaii* (Palo Alto: Pacific Books), pp. 66 and 103.

Strom, R. G. 1964, "Analysis of Lunar Lineaments. I: Tectonic Maps of the Moon," in *LPL Comm.* No. 39, **2**, 205–216.

Tazieff, H. 1970, "The Afar Triangle," *Scientific American,* **222**, No. 2, p. 38.

Turner, R. 1966, "Model of Area Near Ranger VII Impact Site: Additional Views" in "Interpretations of *Ranger VII* Records," Appendix A, *LPL Comm.* No. 58, **2**, 65–68. Cf. also reproductions of *Ranger IX* models by author in Kuiper *et al.,* 1966, pp. 120–129.

Whitaker, E., Kuiper, G. P., Hartmann, W. K., and Spradley, L. H. 1963, *Rectified Lunar Atlas. Supplement No. 2 to the Photographic Lunar Atlas,* Contri. LPL No. 3 (Tucson: University of Arizona Press), p. 6.

APPENDIX I

The Tycho Rim Model and the "Pebble" *by* GERARD P. KUIPER

Through his model of the Tycho rim section, Mr. Turner has demonstrated that *it is possible to derive numerical information on elevations and general topography by the projection methods* he has devised. By recreating the conditions of illumination of the available *Orbiter* records and supplementing them with existing and newly-derived telescopic records, he has found it possible to integrate all topographic and albedo information of the area into a single realistic model. The Topographic *Map A* and the Relief Contour *Map B* summarize in readily accessible form the results of his painstaking work.

The Tycho rim area was selected by this Laboratory for detailed study because of its obvious scientific interest. The discovery of lava lakes in the rim of Alphonsus crater (JPL-NASA *Ranger VIII-IX* Report, 1966, pp. 43 and 137) had provided new insights into the dynamics of formation of large impact craters. The presence of volcanism induced by the Tycho impact had already been concluded from visual observations in the 1950's and had been frequently discussed since.

I found a seemingly-unique, elongated, white object during a survey with the Mt. Wilson 60-inch telescope in 1956, about 3.4 × 8.7 km in size, 14 km from the Tycho wall, just inside the wall of the neighbor crater Pictet, which in lectures I called the *Pebble* for its overall appearance and shape. It was photographed frequently with the 40- and 82-inch telescopes in the late 1950's under different illuminations and is well shown in the Yerkes Plate No. 160, reproduced in the *Photographic Lunar Atlas* (Chicago 1960), Chart D7d. It is not shown (in shadow) on the ACIC Lunar Chart *LAC 112*. The Pebble is white *before* full moon and is seen bright on the *Consolidated Lunar Atlas,* Charts G11, G13, and G15; and even better on Catalina #4114, reproduced in Mr. Turner's Fig. 30b (5 × 10 mm in size), 2.5 cm south of the model boundary and 2 cm outside the Tycho rim. At full moon and after, the object is much darker; and in the afternoon view, G12 *(op. cit.),* it is dark and barely discernible. These properties were noted also during the visual observations in the 1950's and maximum resolution was sought with the 82-inch telescope. The Pebble was found resting roughly half-way out, on the inner slope of Pictet, at a curious angle, not parallel to the crater rim, as if it had landed there in a random position. Since the dimensions of the object were not unlike those of Apollo-type asteroids, this possibility for its origin was considered at the time. However, visual inspection with the 82-inch under excellent conditions in 1958 disclosed that the east rim of Tycho contained *a number of dark lava patches which suggested that the entire area was affected by volcanism induced by the Tycho impact.* It was noted that the Pebble was *roughly parallel to the Tycho rim,* and therefore *probably caused by the Tycho impact* and unrelated

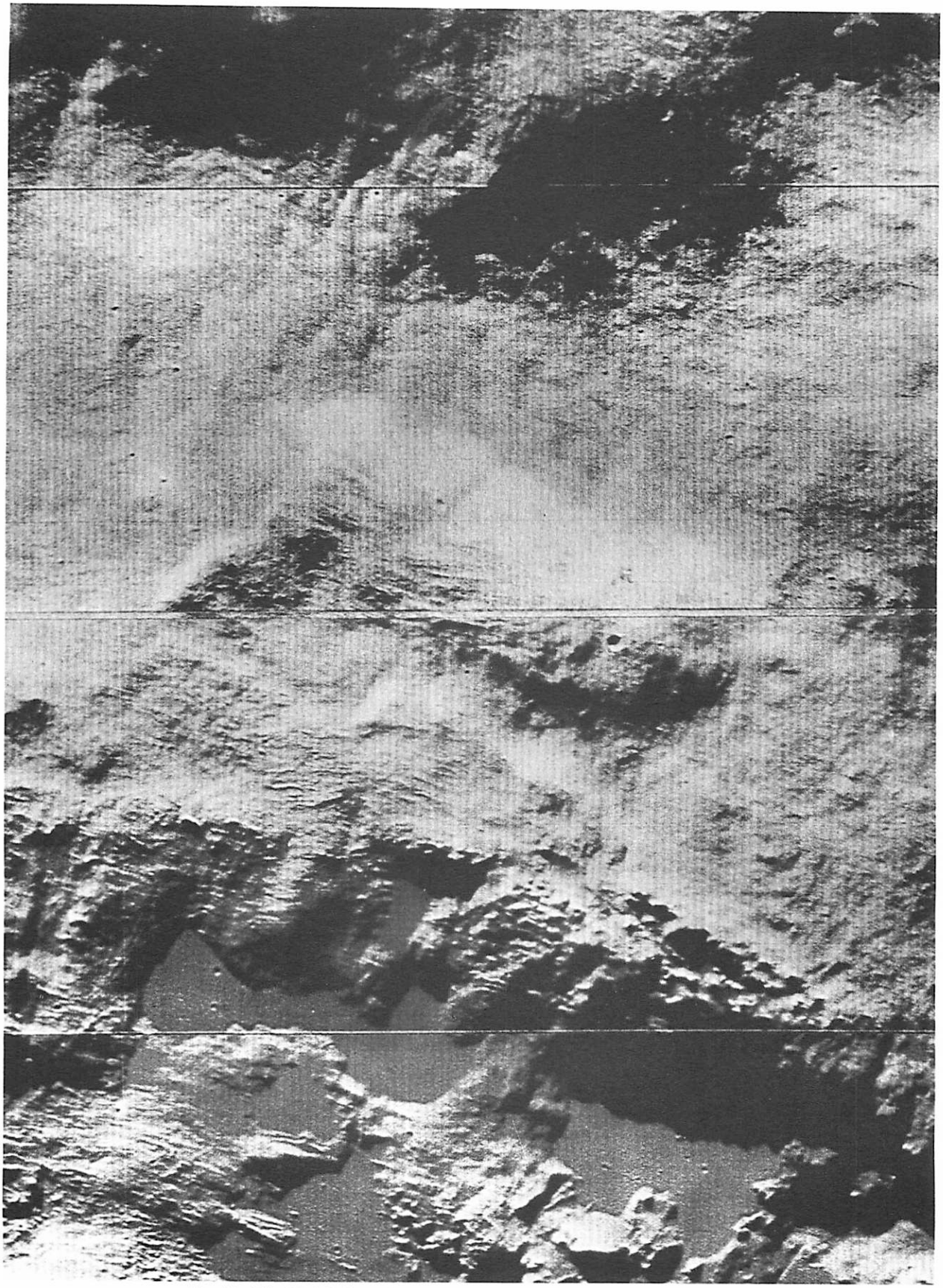

Fig. 33 The "Pebble" and lava lakes in NE Rim of Tycho, *Orbiter V*, M 125.

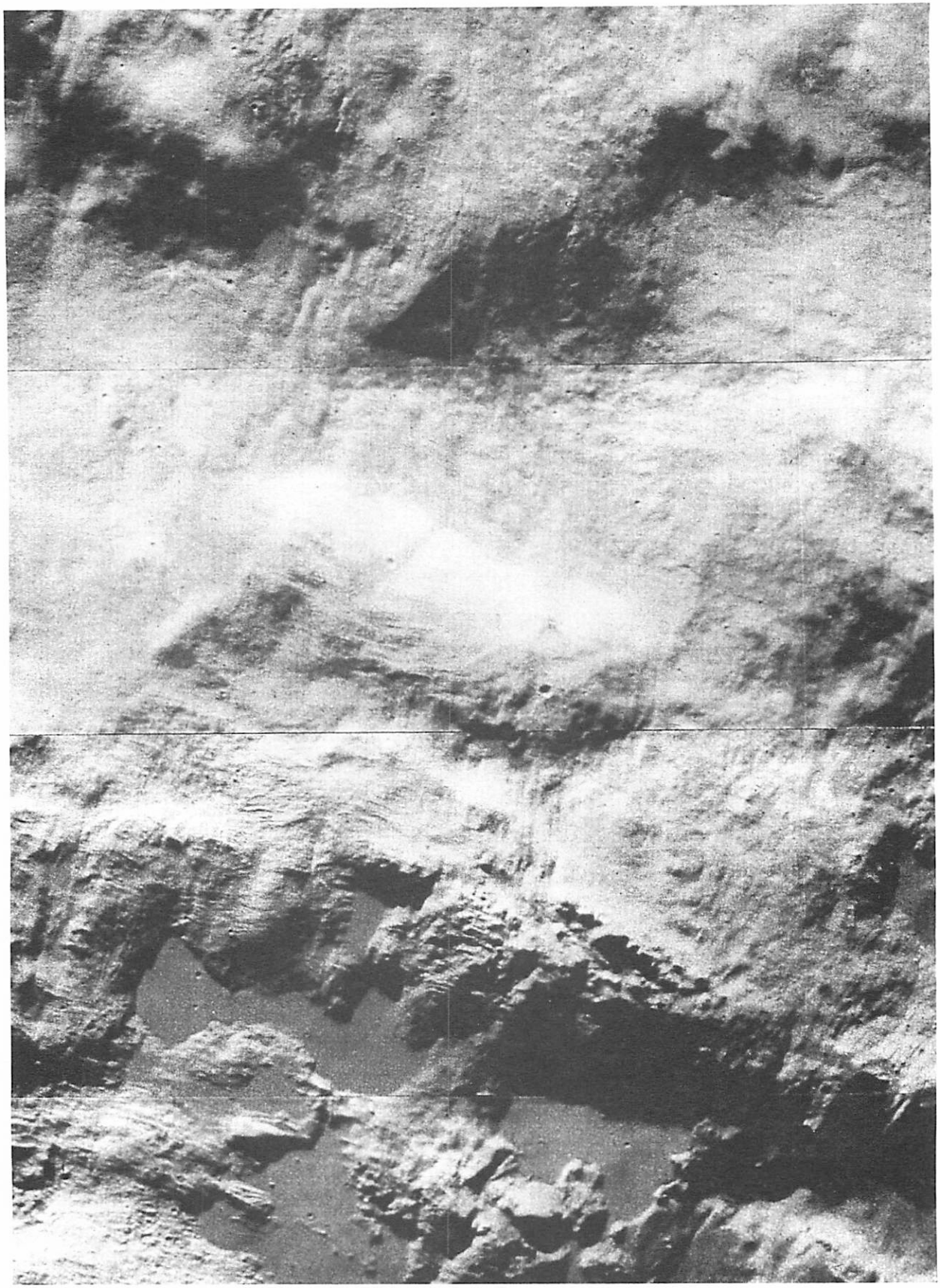

Fig. 34 As Fig. 33, *Orbiter V*, M 126.

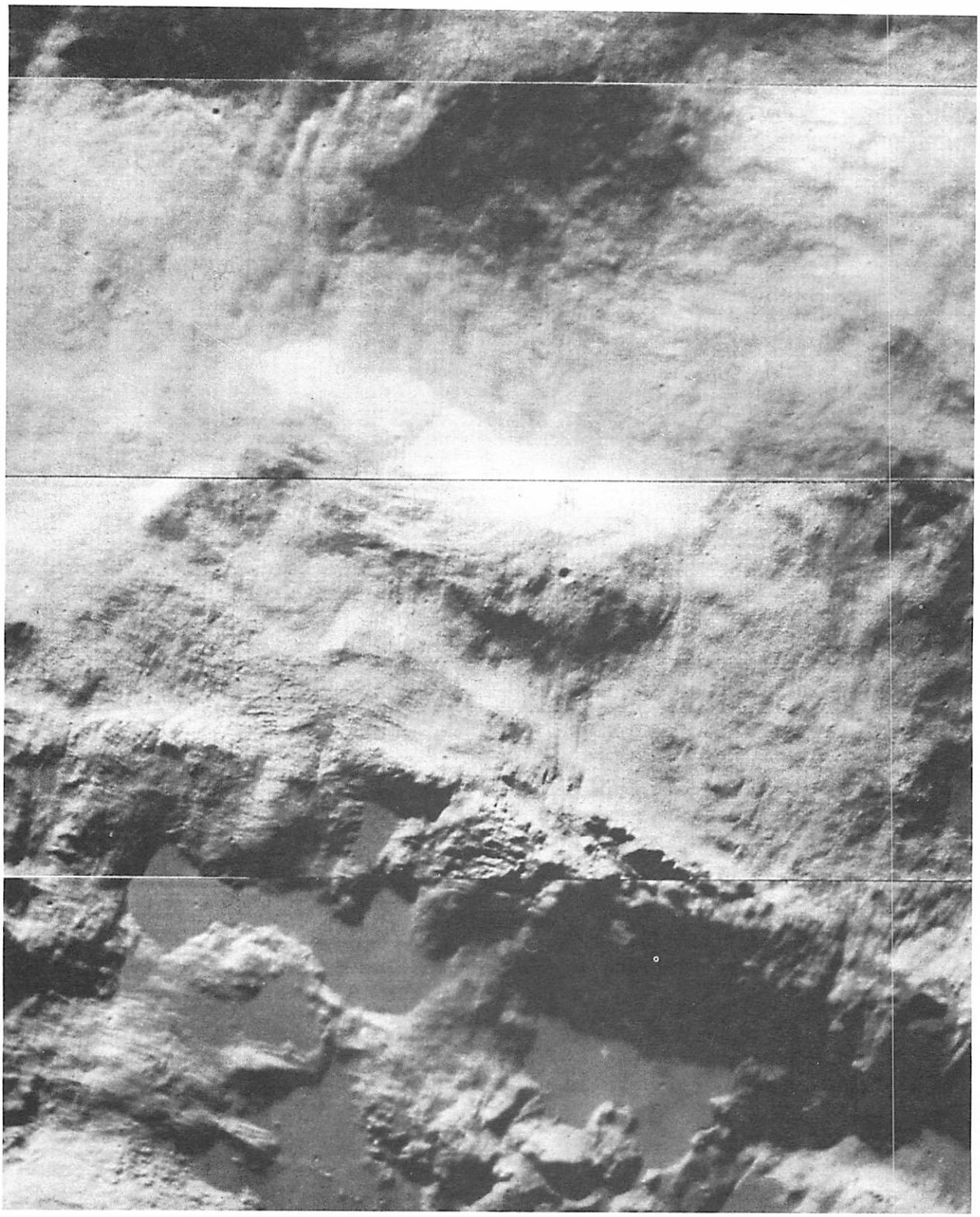

Fig. 35 As Fig. 33, *Orbiter V*, M 127.

to Pictet itself. It was assumed that the dark W side was probably due to lava cover and that the E side resembled the central peak of Alphonsus (taken to be volcanic in origin; Kuiper, 1954, p. 1108). The bright side of the Pebble looked smooth in the telescope, like the Alphonsus peak.

The much higher resolution provided by the *Orbiter* records invites re-examination of the Pebble. It was actually our first incentive for Mr. Turner's Tycho rim study (which will be continued for the adjacent rim area up to and including the Pebble). Pending the completion of this model study, three photographic *Orbiter V* records, M125, 126, and 127, are herewith reproduced (Figs. 33-35) based on "enhanced" positive film copies kindly provided by the NASA Data Center. These records are of extraordinary interest and beauty.

Stereoscopic inspection of these *Orbiter V* records shows that the morning (E.) side of the Pebble is indeed of high albedo and that part of the top and the entire W side are covered by a complex system of lava flows, apparently originating in fissures and some volcanic mounds, well shown on the photographs. A small lava pool is seen in full sunlight at the foot of the west slope of the Pebble, as dark as the larger lava lakes nearby (cf. M 126). Seen stereoscopically, the larger lakes on the Tycho rim show various levels, similar to those farther north, in Mr. Turner's model; the small rectangular lake nearest the Pebble is the highest.

The Pebble still seems unique on the Moon, not being near-central to an impact area, but peripheral. It lacks the simple symmetry of the Alphonsus central peak and it is not obvious that its entire volume is due to volcanism.

REFERENCE

Kuiper, G. P. 1954, "On the Origin of the Lunar Surface Features," *Proc. of the Natl. Acad. of Sci.*, 40, pp. 1096–1112.

APPENDIX II

Tycho Crater Statistics

by C. A. WOOD AND W. K. HARTMANN

The diameter distribution of craters larger than 60 m diameter in the area of Turner's model is shown in Fig. 36. It was necessary to consult all four *Orbiter* photographs to detect all craters, and care was taken to correct for shadowed and burned-in areas of the photographs. These counts were used to date Tycho in two ways: (1) the crater density was divided by the cratering rate for craters in the appropriate size

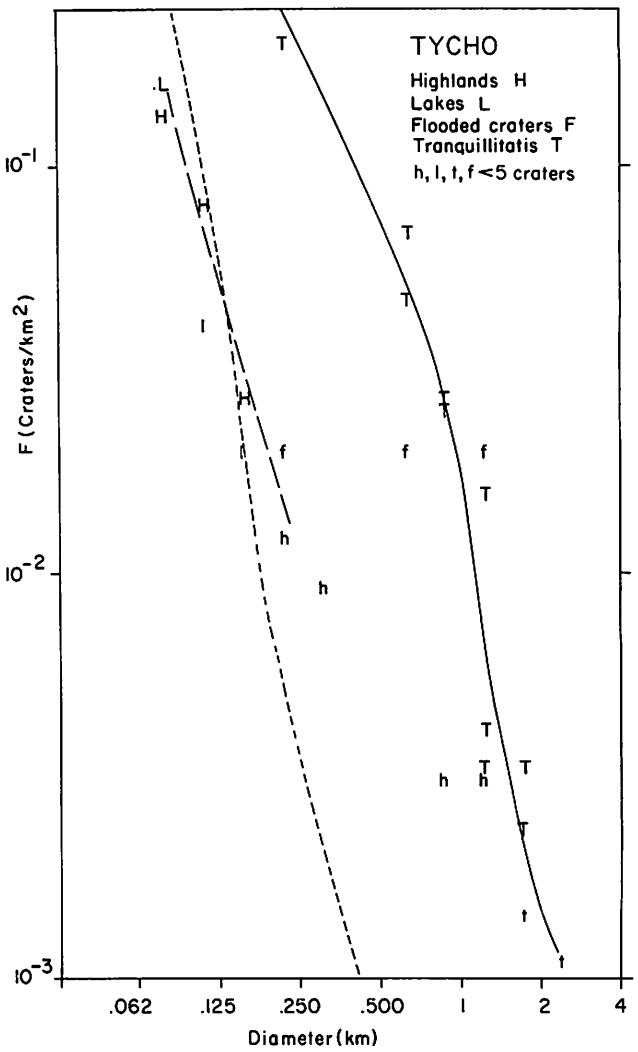

Fig. 36 Crater counts in the area of Turner's Tycho model, based on medium-resolution *Orbiter* photographs. Dashed line shows curve of slope −2 fitted to observed crater counts. Dotted line shows earlier curve based on data published by Strom and Fielder (1968) and Hartmann (1968). Solid line shows Mare Tranquillitatis for comparison.

range, using Vedder's (1966) compilation of meteorite fluxes. There is about a factor of 3 uncertainty in these fluxes. The resulting age is 7.0×10^8 yrs; (2) the crater density was compared with the crater densities found in the *Apollo 12* area, recently reported to be 3.4×10^9 yrs in age. The relative density of craters on Tycho's rim is about 0.06 that of the *Apollo 12* region (which in turn has a crater density .75 times the "normal" mare), giving a scaled age of 2.7×10^8 yrs, under the assumption of a constant cratering rate since Oceanus Procellarum formed. This method is not as reliable as the first method due to uncertainties in cratering history, relative crater densities, and possible contamination

by endogenic or secondary craters. If the lead-lead dating (4.2×10^9 yrs) of the Mare Tranquillitatis rocks is used instead, the scaled age of Tycho is 1.6×10^8 yrs.

These ages agree well with those derived independently by Strom and Fielder (1968) and Hartmann (1968), i.e. about 2×10^8 yrs.

The crater counts show marginally fewer craters in the "lakes" than in the immediately surrounding uplands, indicating they formed at nearly the same time. On the other hand, Strom and Fielder, on the basis of the high-resolution photography on the N rim, concluded that the "lakes" are significantly younger than Tycho. "Pre-lake" craters larger than 700 m diameter show through the lava, indicating a probable depth of lava of a few hundred meters. The highland region contains few older craters and seems to have been smoothed and coarsely grooved, perhaps by base-surge activity associated with the formation of Tycho.

REFERENCES

Hartmann, W. K. 1968, "Lunar Crater Counts. VI: The Young Craters Tycho, Aristarchus, and Copernicus," *LPL Comm.* No. 119, **7**, 145–156.

Strom, R. G., and Fielder, G. 1968, "Multiphase Development of the Lunar Crater Tycho," *Nature,* **217**, 611–615.

Vedder, J. F. 1966, "Minor Objects in the Solar System," *Space Science Reviews,* **6**, 365–414.

APPENDIX III

Dimple Craters on Moon and Earth
by RALPH J. TURNER

One of the most interesting discoveries in NASA's *Ranger* Program is the presence of thousands of so-called dimple craters on the Moon. These have been attributed by Kuiper *et al.* (1966, p. 80) to a special kind of collapse depression, different from the wider class of collapse depressions that exhibits near-circular flat bottoms and gentle slopes without elevated rims, ranging in diameter from less than 100 m to several km. The dimple craters have somewhat pointed centers, sometimes elongated in the form of a crease. At the suggestion of Dr. Kuiper, the author made a model study of one lunar dimple crater and a detailed comparison with a terrestrial analogue of the type already described in the *Ranger IX* Report *(op. cit.* pp. 81–88), which also illustrates a good selection of additional lunar dimple craters. Fig. 37 portrays the dimple crater selected *(op. cit.* p. 93) as recorded by *Ranger VIII* with *east* illu-

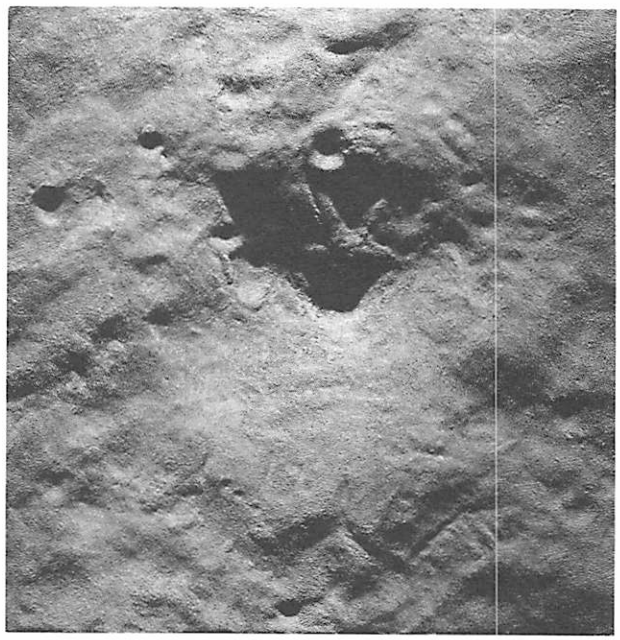

Fig. 37 Model of a dimple crater in Mare Tranquillitatis under illumination simulating *Ranger VIII* illumination conditions (14°.5 ⊙ altitude, east illumination).

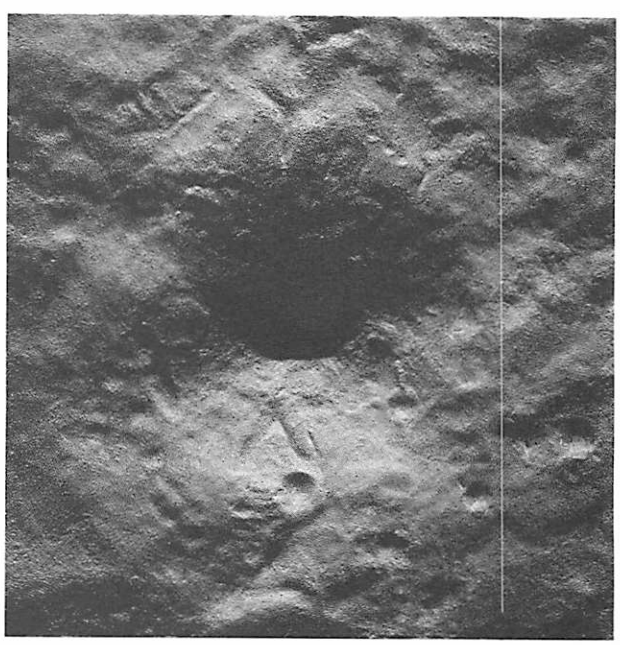

Fig. 38 Model of Tranquillitatis crater under west illumination (⊙altitude 14°.5).

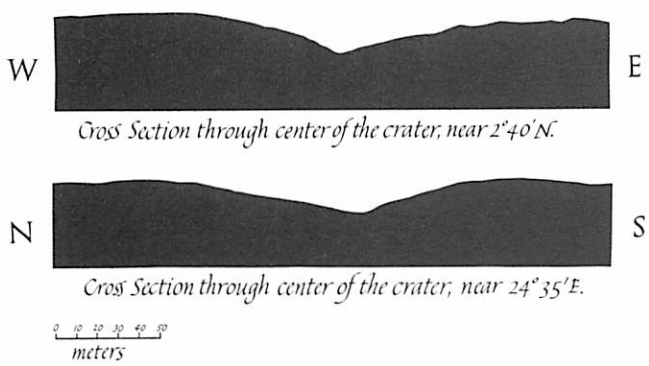

Fig. 39 Cross section of Tranquillitatis crater taken from the relief model.

Fig. 40 Carrizozo Lava flow collapse crater model (⊙ altitude 33° east illumination).

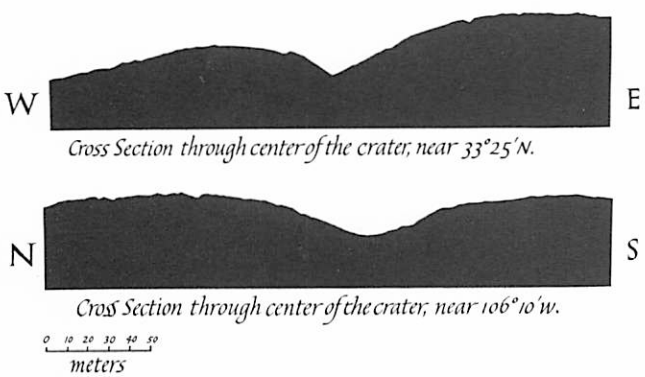

Fig. 41 Cross sections of the Carrizozo crater from a survey in the field and the model.

mination and sun elevation 14°5. The model under a *W* illumination, with the same sun elevation, is shown in Fig. 38. Fig. 39 shows two cross sections of the model, one E-W, the other N-S.

The terrestrial comparison is shown in Fig. 40, with the two cross sections in Fig. 41. The dimple crater modeled is the one shown on Fig. 42 of the NASA-JPL *Ranger VIII-IX* Report, in the left margin of the photograph, which also contains a scale in meters; and on Fig. 43 *(op. cit.)* in the lower right-hand margin, 3.5 cm from the right edge. The correspondence between Fig. 40 and the numerous tension cracks on the lava field in the two records is found readily. The absence of the small tension cracks around the lunar dimple crater may be attributed to differences in the texture of the upper meter or 2 of the lunar lavas (solidified under vacuum conditions); and micro-meteorite impact since the formation of the mare some 4 billion years ago. The terrestral tension cracks are instructive of the process of dimple-crater formation, already briefly reviewed in the *Ranger* Report.

REFERENCE

Kuiper, G. P., Strom, R. G., and Le Poole, R. S. 1966, "Interpretation of the *Ranger* Records," in *Ranger VIII* and *IX. Part II. Experimenters' Analysis and Interpretation,* JPL Tech. Report No. 32-800, pp. 35–248.